Development of time-dependent reaction rates to optimize predictor-corrector algorithm in ALEPH burn-up tool

Mr. Luca Fiorito

Academic year 2011-2012

Promotor: Pr. Dr. Ir. Pierre-Etienne Labeau, ULB

Thesis submitted in partial fulfilment of the requirements for the degree of Master of Science in Nuclear Engineering

Belgian Nuclear Higher Education Network, c/o SCK•CEN, Boeretang 200, BE-2400 Mol, Belgium

Master of Science in Nuclear Engineering

Thesis Summary Page

Name of the student:

Luca Fiorito

Title:

Development of time-dependent reaction rates to optimize predictor-corrector algorithm in ALEPH burn-up tool

Abstract:

Shells coupling Monte-Carlo transport and deterministic depletion codes are extensively used within the nuclear field to simulate material changes throughout irradiation. The dynamic of the phenomenon is described by the system of coupled ordinary differential equations with a generally stiff matrix of the coefficients. Matrix coefficients represent decay constants and microscopic reaction rates of the numerous nuclides involved in the calculations. Current codes solve the system depleting the fuel by using constant matrix coefficients. For a typical burn-up problem, the most of the time is consumed by the calculation of these neutronic coefficients, while only a small fraction is used by the depletion solver. Recently, predictor-corrector methods and other techniques have been implemented to guarantee more accurate results.
This thesis work presents the unique and innovative feature of depletion codes to better optimise the predictor corrector algorithm by using time-dependent matrix coefficients when solving the system of ODE's. Linear polynomials interpolate the evolution of the matrix coefficients along a few consecutive time steps. They allow to extrapolate the effective reaction rates of the following steps reducing the required computational time spent in the neutronic calculation and granting a slight improvement in the accuracy of the results, as well. In this thesis work, this technique has been tested, in combination with the version 2 of the ALEPH Monte-Carlo burn-up code, on the REBUS experimental benchmark and simulating irradiation of the MYRRHA critical core configuration.

Promotor: Pr. Dr. Ir. Pierre Etienne Labeau Approval for submission by promotor:

Mentor: Dr. Alexey Stankovskiy

Assessors: Pr. Dr.Ir. Gert Van den Eynde
Pr. Ir. Hubert Druenne
Pr. Dr. Ir. Sandra Dulla

Academic Year 2011 - 2012.

Copyright

The author and promoter grant permission to make this thesis available for consultation and copy parts for personal use. Every other use is subject to the limitation of copyright, in particular the obligation to explicitly mention the source when referring to the content of this thesis.

© BNEN, Belgian Nuclear higher Education Network[1]

[1] BNEN is a consortium of the Belgian universities *Katholieke Universiteit Leuven (K.U.Leuven), Université catholique de Louvain (UCL), Université de Liège (ULg), Universiteit Gent (UGent), Vrije Universiteit Brussel (VUB), Université Libre de Bruxelles (ULB)* in collaboration with the *Belgian Nuclear Research Centre SCK•CEN.*

Administration Manager BNEN: Thomas Berkvens, bnen@sckcen.be, c/o SCK•CEN, Boeretang 200, B-2400 MOL, Belgium.

Table of Contents

Abstract

Shells coupling Monte-Carlo transport and deterministic depletion codes are extensively used within the nuclear field to simulate material changes throughout irradiation. The dynamic of the phenomenon is described by the system of coupled ordinary differential equations with a generally stiff matrix of the coefficients. Matrix coefficients represent decay constants and microscopic reaction rates of the numerous nuclides involved in the calculations. Current codes solve the system first calculating the nuclear parameters using a steady-state Monte-Carlo particle transport code and then depleting the fuel along several time steps. For a typical burn-up problem, the most of the time is consumed by the neutronic calculation, while only a small fraction is used by the depletion solver. Recently, predictor-corrector methods and other techniques have been implemented to guarantee more accurate results. One has to predict the development of the reaction rates during the step and then further correct these predictions to deplete the material. However, these methods tend to slow down the code because of the continuous neutronic computation.

This thesis work presents the unique and innovative feature of depletion codes to better optimise the predictor corrector algorithm by using time-dependent matrix coefficients when solving the system of ODE's. Linear polynomials interpolate the evolution of the matrix coefficients along a few consecutive time steps. They allow to extrapolate the effective reaction rates of following steps avoiding the cumbersome launch of Monte-Carlo stochastic codes. This greatly reduces the required computational time and grants a slight improvement in the accuracy of the results, as well. In this thesis work, this technique has been tested, in combination with the version 2 of the ALEPH Monte-Carlo burn-up code, on the REBUS experimental benchmark and simulating irradiation of the MYRRHA critical core configuration.

List of abbreviations

ADS	Accelerator Driven System
BDF	Backward Differentiation Formulas
BR2	Belgian Reactor 2P
BOC	Beginning Of Cycle
BOS	Beginning Of the Step
CANDU	CANada Deuterium Uranium reactor
CE	Constant Extrapolation
CRAM	Chebyshev Rational Approximation Method
EOS	End Of the Step
GEN IV	GENeration 4
HM	Heavy Metal
IRK	Implicit Runge-Kutta
JEFF	Joint Evaluated Fission and Fusion Library
LBE	Lead-Bismuth Eutectic
LE	Linear Extrapolation
LI	Linear Interpolation
LINAC	LINear ACcelerator
LWR	Light Water Reactor
MCNP	Monte Carlo N-Particle transport code
MCNPX	Monte Carlo N-Particle eXtended transport code
MYRRHA	Multi-purpose hYbrid Research Reactor for High-tech Applications
MOX	Mixed Oxide fuel
ODE	Ordinary Differential Equation
PWR	Pressurized Water Reactor
QI	Quadratic Interpolation
RMSD	Root-Mean-Squared Deviation
RR	Reaction Rate
SBU	Seed Blanket Unit
SCRAM	Safety Control Rod Axe Man
TDM	Time-Dependent Matrix
TTA	Transmutation Trajectory Analysis

Chapter 1

Introduction

1.1 Monte-Carlo burn-up codes

All nuclear systems, from the present commercial reactors to the future designs, require a complete and reliable isotopic inventory prediction for aspects related to safety, operation and waste management purposes. Therefore, being able to accurately solve variations in compositions of materials under irradiation and/or undergoing decay has become of primary importance. In addressing this problem, appropriate burn-up calculation codes (also known as depletion, or inventory codes) have been developed. These solvers aim at following the time development of material composition and neutronic parameters of a nuclear facility. The spread of coupled Monte-Carlo burn-up codes came along together with the growth of computing power that allowed a wide share and development in nuclear reactor applications and nuclear criticality research. In this sense, the Monte-Carlo burn-up code ALEPH is being developed in SCK•CEN since 2004 [1]. However, since already 30 years ago, stochastic transport codes have been coupled with material depletion solvers. Indeed, the Monte Carlo particle transport code MCNP [2] has been linked with the one-group depletion code ORIGEN [3] in automatic running programs such as MCODE [4], MONTEBURNS [5] or MCOR [6]. The ALEPH code figures in this list, as it combines any version of MCNP or MCNPX [7] [8] Monte-Carlo radiation transport with the ORIGEN-2.2 [3] depletion code, or the RADAU5 module [9] – which uses an implicit Runge-Kutta method (Radau IIA) of order 5 (three stages) with step size control and continuous output – in the new version ALEPH2 [10].

1.2 Stochastic and deterministic

A burn-up Monte-Carlo code merges the potentialities of a stochastic Monte-Carlo transport code and a deterministic solver. The Monte-Carlo tool solves the Boltzmann transport equation by stochastic Monte-Carlo method which owes the accuracy of its results to the quantity of input data introduced in the calculation, that is, the amount of histories simulated to derive the statistical behaviour of the system. The Boltzmann equation reproduces the flux spectrum of neutrons in a local form. It is solved by stochastic codes since they can provide the most accurate locally dependent spectra and fluxes in realistic three-dimensional geometry. Moreover, it can also provide answers in areas where traditional deterministic codes are lacking.

Monte-Carlo codes reproduce the spectrum calculation even in complex full 3D geometry, but they show evident limits in applicability to follow the time-dependent behaviour of the neutronic parameters. Therefore, depletion solvers have been developed worldwide to simulate the burn-up evolution in time expressed as the change in nuclide concentrations. Amongst them, several tools can be mentioned like CINDER'90 [11] and ORIGEN, however some codes use built-in burn-up depletion modules as MCB [12] or the CRAM [13] algorithm of SERPENT [14]. The deterministic solver duty is to compute the dynamic evolution of the isotopic inventory throughout the burn-up period. Numerical methods are extensively used for these calculations, such as the matrix exponential method in ORIGEN-2.2. In the SCK•CEN context, the RADAU5 module was recently added to the ALEPH code – it solves the depletion system by using an implicit Runge-Kutta method of order 5.

1.3 Computational time

Burn-up codes follow the depletion of nuclide concentrations under irradiation, these calculations are influenced by several factors responsible for as many difficulties. The dynamic evolution of the irradiated material is described by a first order system of differential equations, where the governing parameters, clustered in a square sparse matrix, are half-lives and transmutation cross sections of the several isotopes. The irradiated nuclear fuel contains thousands of different nuclides with widely varying half-

lives, resulting in an extremely large and stiff matrix. Besides, the neutron flux and the other neutronic properties – spectra and fission products yields – are strongly dependent on the isotopic compositions and therefore they affect each other leading to complex combined problems. Since burn-up calculations focus on long-term changes of irradiated materials, this issue is usually overcome by solving neutronics and variations of material compositions in sequence, while assuming every time the other to remain constant. This procedure is extensively used in the most of the currently available burn-up codes. However, adopting such codes a main drawback is encountered, that makes them weak on the computational time consumption point of view, or subject to further improvement.
The two parts the code is divided into are respectively steady-state, as long as the neutronic calculation is concerned, and time-dependent in the depletion part. The difference in running time between the two subdivisions is remarkable: for a typical burn-up computation most of the time is spent to perform the neutronics, while only several percents of the total time are used to deplete the material. This is just a rough and general reflection based on observations carried out during this thesis work – other models with a lot of material to follow may adjust the time proportion in a different way – anyway it can be considered the customary relation.
This work aims at overcoming the time consumption problem by modifying the nature of the solution procedure. The Monte-Carlo steady-state part is assumed dependent on time to better reproduce the stiffness of the matrix. The selected method makes use of polynomial functions to interpolate and then extrapolate the matrix coefficients along the time intervals, in order to skip the time-expensive Monte-Carlo transport part. The foreseen results expect a higher accuracy on the isotopic inventory at the end of calculations due to the improved reproduction of the matrix evolution in time. Moreover, since MCNP calculations are severely reduced in number, the computational time is supposed to outstandingly decrease.

Chapter 2

Methodology

2.1 The ALEPH code

The common principle of Monte-Carlo depletion codes is to perform a steady-state Monte-Carlo particle transport calculation to compute the neutron flux distribution. The second step follows up and occurs in the depletion of the material by solving the stiff system of ordinary differential equations for a given time span using reaction rates obtained from calculated fluxes and spectra. This procedure repeats up to the end of the irradiation history.

The ALEPH code, developed and validated in SCK•CEN, was initially only able to perform burn-up calculations for typical reactor systems. However, the recently applied refurbishment made it really general-purpose [15] [10], or versatile, such that a wide range of problems can be modelled. Amongst the several purposes, ALEPH is currently being extensively exploited, in its in-house use, for depletion and activation calculations of the MYRRHA project.

The Multi-purpose Hybrid Research Reactor for High-tech Application (MYRRHA) is a nuclear reactor projected by the Belgian Nuclear Centre SCK•CEN in Mol and currently in the designing phase [16]. It is based on the Accelerator-Driven System (ADS) concept and it is assumed it can operate both in sub-critical and critical modes. The performance of neutronic design for this system requires dedicated codes. As a matter of fact, the majority of neutron transport codes used in the analysis of critical systems cannot fit ADS calculations since the multi-particle physics for this design extends far beyond the

typical energy range actual commercial reactors deal with. Therefore, amongst the extended number of *N*-particle Monte-Carlo transport code, MCNP(X) is the only one that possesses the ability to treat such problems, like ADS-related systems. Its full capability rises from its proficiency in tracking almost all particle types of nearly whatever energy considered. However, no depletion code, but ALEPH, can account of proton induced reactions, which play an important role in the activation of spallation target and nearby structure – not even those which can use MCNP(X), or MCNP(X) itself with its depletion capability. Hence, ALEPH is advertised as a unique code which is able to carry such type of calculations by using proton induced cross sections.

What makes ALEPH very unique, within the category of shells coupling Monte-Carlo transport and deterministic depletion codes, are some very distinctive features that distinguish it from the crowd. ALEPH possesses full consistency of cross section data, which allows it to use the same unionized cross section tables, linearised on the same energy grid, both for the Monte-Carlo transport step and the subsequent depletion solution.

The new version of the code – ALEPH 2.1 – was released in 2011. In this new edition, ALEPH2 has been set free from the limitation of the previous depletion solver ORIGEN-2.2 by replacing it with the advance built-in depletion module RADAU5. Moreover, the predictor-corrector mechanism was enabled and the nuclear data set extended. These and other modifications caused ALEPH to become a top-flight code in its field.

This thesis intends to describe the work and the tests elaborated to further implement ALEPH2 in the sense of a possible application of time-dependent matrixes of the coefficients when solving the system of ODE by means of the RADAU5 module.

2.2 Burn-up time step

The irradiation history wherein the burn-up calculation is performed embodies both the irradiation cycles and, if present, the decay periods when the power goes to zero and the decay of radioactive species is the only parameter affecting the depletion. The neutron transport equation for the typical burn-up problem is solved in steady-state conditions, introducing nuclear cross section data and neutron yields per fission that, in turn, are calculated by referring to the isotopic densities present in the core at the time of the

computation. To carry out a burn-up calculation, the whole burn-up period may be divided into several consecutive time intervals *dt*. Along each time span the neutron flux is supposed to be as more constant as possible, therefore, every interval is tailored such that this condition is to a first order satisfied. The constant assumptions come in useful to get accurate results of the system of ordinary differential equations, or ODE's. The reaction rates of the stiff matrix *A* in the first-order depletion system are directly obtained from the steady-state solution of the transport equation. Therefore, since the subsequent neutronic calculation occurs at the end of the step (EOS) after the material exhaustion, the current numerical depletion codes solve the system using the retrieved values of reaction rates calculated at the beginning of the step (BOS), keeping them constant throughout the all time step. It is clear that a big variation of neutronic parameters within a single time interval gives experimental depletion solutions that are far from being suitably simulated by using constant reaction rates generated with steady-state Monte-Carlo method.

Hence, the splitting of the burn-up irradiation or decay interval in several substeps is indeed performed to guarantee consistency and adequate results.

2.3 The ALEPH scheme

A typical ALEPH calculation starts with the processing of the input file. An ALEPH input file is generally straightforward and easily comprehensible, it enwraps the MCNP(X) input file and requires only some extra cards. These features render the code very easy to use. Then, ALEPH builds a new MCNP(X) input file based upon the input options of the user and starts the MCNP(X) calculation. The MCNP(X) tool performs the stochastic Monte-Carlo calculation and retrieves the neutron spectra and flux distribution in every burn-up zone at time $t=t_0$, identified as the beginning of the burn-up analysis. Afterwards, the neutron spectra, in combination with the nuclear data library, collapse the total spectral-averaged single-group microscopic cross sections and the integrated flux. The method used to calculate the reaction rates $\bar{\sigma}\bar{\phi}$ is an optimal, highly accurate multi-group binning approach, whereas the one-group averaged flux is computed normalising onto the power, or set directly by the user, normalising onto the results of suitable selected tally requested in the MCNP(X) part of the input file [10]. Reaction

rates are then uploaded in the built-in solver of the system of ordinary differential equations that models the dynamics of the isotopic inventory evolution throughout the time step. In essence, the module solves the system $\frac{d\vec{N}(t)}{dt} = A\vec{N}(t)$, where N is the vector of nuclide concentrations and A is the generally stiff square matrix of the coefficients. Each coefficient comprehends the sum of decay constants of nuclide j into nuclide i plus the reaction rate to produce nuclide i from nuclide j by nuclear reaction. In the current implementation of ALEPH, these reaction rates are calculated at the beginning of each time interval and are assumed to be constant during the time step dt.

After the depletion calculation, ALEPH stores the new compositions and passes them on either to build a new MCNP(X) input file for the further irradiation step or immediately to solve the concentrations for a new time step if the decay of the materials is requested. In the new version ALEPH2, the code gives the user the possibility to choose whether to apply or not the predictor-corrector method before passing on to the next step. The current ALEPH2 scheme is reported in Fig. 1.

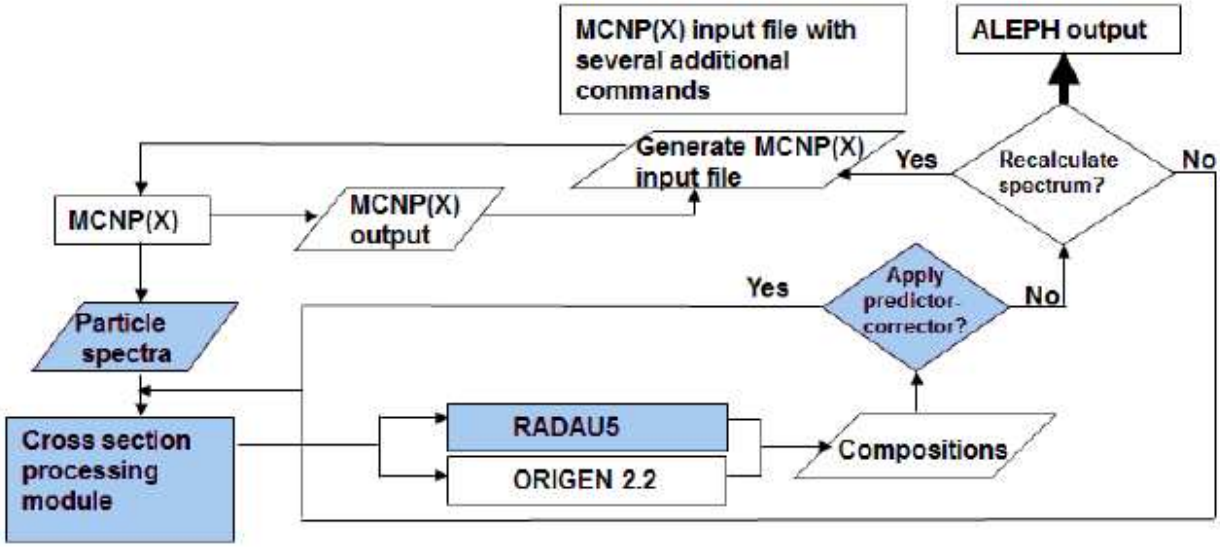

Figure 1: Flowchart of ALEPH2.

2.4 The evolution of material subject to irradiation

Materials subject to radiation in an irradiating environment, like a nuclear reactor core, undergo a series of transmutations that depends on the energies and particles involved in

the collisions. The result is a variation of the concentrations in the irradiated fuel, followed by generation of new nuclides.

In a nuclear reactor, the material undergoing depletion usually loaded in LWR's is UO_2 or a mixture of U and Pu in oxide form. The latter is also called MOX fuel and generally shows an amount of Pu of 10 wt%. In addition, fuel rods enriched with Gd in the order of 5-12 wt% are frequently adopted to limit the reactivity and power peaking factors in hot spots. Uranium is ordinarily enriched up to 5 wt% in U-235 – according to the Belgian legal limit for commercial nuclear reactors. Other kinds of reactors are allowed to use high-enriched fuel for testing and experimental purposes and for prototypes, whereas natural uranium (x=0.072 wt%) is used in CANDU's and some other types of reactors. Also metallic uranium is frequently handled, especially in gas moderated nuclear reactors, while several different experimental fuels are spreading with the coming of GEN IV reactors. The Belgian Materials Testing BR2 facility in SCK•CEN, for instance, burns 93 wt% enriched uranium in the metallic form UAl and neutrons are moderated by a matrix of beryllium and cooled by light water [17].

In colliding with the fuel, neutrons and other particles initiate several reactions: scattering, capture, fission and so on. Particle captures, as well as fission reactions, transmute initial materials to final states that account in the depletion of the burn-up calculation. In addition, since the material is radioactive, the decay inherent feature has to be considered, too. The evolution of a material subject to radiation is described by a system of coupled linear differential equations. Bateman showed that the analytical solution of these kinds of system is possible when only one nuclide has non-zero initial concentration. A general ODE system for reactor problems has a lot of non-zero concentrations; therefore, strictly speaking, the treated systems cannot be called systems of Bateman equations. However, for historical reasons, it is common practice to do it [18]. For a particular nuclide *i*, these equations can be written in their most general form [19] as

$$\begin{aligned}\frac{d}{dt}n_i(\vec{r},t) &= \sum_{j\neq i} L_{ij}\lambda_j n_j(\vec{r},t) - \lambda_i n_i(\vec{r},t) \\ &+ \sum_{j\neq i}\sum_{r}\int n_j(\vec{r},t)Y_{ij,r}(E)\sigma_{j,r}(E)\phi(\vec{r},E,t)dE \\ &- \sum_{r}\int n_i(\vec{r},t)\sigma_{i,r}(E)\phi(\vec{r},E,t)dE\end{aligned} \qquad (1)$$

where

n_i = atomic density of nuclide *i*

λ_i = total decay constant of nuclide *i*

L_{ij} = decay branching ratio of nuclide *j* to nuclide *i*

$Y_{ij,r}$ = yield of nuclide *i* for reaction *r* on nuclide *j*

$\sigma_{i,r}$ = microscopic cross section of nuclide *i* for a reaction *r*

ϕ = scalar neutron flux

The equation can be cast in a more compact form:

$$\frac{d}{dt} n_i(t) = \sum_j A_{ij}(t) n_j(t) \qquad (2)$$

where

$$A_{ij}(t) = \begin{cases} L_{ij}\lambda_j + \sum_r Y_{ij,r}(t)\sigma_{j,r}(t)\phi(t) \\ \lambda_i - \sum_r \sigma_{i,r}(t)\phi(t) \end{cases} \qquad (3)$$

ALEPH averages the nuclear parameters in equation (3) over the spectrum in a single energy group, resulting in the spectral-averaged one-group flux $\phi(\vec{r},t)$, yields $Y_{ij}(\vec{r},t)$ and one-group averaged cross sections $\sigma_{ij}(\vec{r},t)$. Besides, when running the transport calculation, within each burn-up zone the material composition is considered spatially constant and the particle flux and spectrum are assumed to be fixed during the evolution calculation. The previous quantities can thus be spatially averaged in each burn-up zone:

$$\phi(t) = \frac{\int\int \phi(\vec{r},E,t)\,dE\,dV}{\int dV} \qquad (4)$$

$$Y_{ij,r}(t) = \frac{\int\int Y_{ij,r}(E)\sigma_{j,r}(E)\phi(\vec{r},E,t)dEdV}{\int\int \sigma_{j,r}(E)\phi(\vec{r},E,t)dEdV} \quad (5)$$

$$\sigma_{i,r}(t) = \frac{\int\int \sigma_{j,r}(E)\phi(\vec{r},E,t)dEdV}{\int\int \phi(\vec{r},E,t)dEdV} \quad (6)$$

The time-dependence is removed since the neutron flux spectrum is calculated by using a steady-state Monte-Carlo tool. Hence, a stochastic code such MCNP(X) estimates the previous integrals during the particle simulation process using the track length estimator, that is, by summing over all tracks *t* going through the cell of interest:

$$\int\int \sigma_{i,r}(E)\phi(\vec{r},E)dEdV = \frac{1}{N_h}\sum_t l_t w_t \sigma_{i,r}(E_t) \quad (7)$$

and

$$\int\int \phi(\vec{r},E)dEdV = \frac{1}{N_h}\sum_t l_t w_t \quad (8)$$

where N_h is the total number of source particles simulated and E_t is the energy of a particle track within the cell with a corresponding track length l_t and weight w_t.
The reaction rates are so calculated multiplying the retrieved value of the flux by the respective averaged cross section.

$$RR_{ij} = \overline{\sigma}_{ij}\overline{\phi} \quad (9)$$

Therefore, assuming that the particle spectra and fluxes remain constant during the time step and locally in the selected volumes, the atom densities of nuclides can be obtained at the end of the time step by solving the system of ordinary differential equations that can be written using a constant matrix *A*:

$$\frac{d}{dt}\vec{N}(t) = A\vec{N}(t) \tag{10}$$

where the matrix coefficients are the transmutation rate of nuclide *i* from nuclide *j*, plus the disappearance rate of nuclide *i*:

$$a_{ji} = \sigma_{ji}\phi + \lambda_{ji} \tag{11}$$

and

$$a_{ii} = -\sigma_i\phi - \lambda_i \tag{12}$$

2.5 Depletion solvers

The previous version 1 of ALEPH solved the depletion part of a burn-up problem using the ORIGEN-2.2 depletion code to obtain the nuclide concentrations at the end of the irradiation step. The algorithm used by ORIGEN-2.2 is the matrix exponential method, where the equation (10), analytically solved, gives the formal solution

$$N(t) = N(0)e^{At} \tag{13}$$

The exponential of the matrix is defined through the Taylor expansion, valid for small times *t*:

$$e^{At} = \sum_{k=0}^{\infty}\frac{1}{k!}(At)^k = I + At + \frac{1}{2}A^2 + \ldots \tag{14}$$

where $A^0 = I$.

A high number of algorithms are nowadays able to compute the matrix exponential solutions, but often they are computationally expensive or of dubious numerical quality.

Hereunder, it has been reported the description of some of the established methods more extensively used in solving burn-up problems.

2.5.1 ORIGEN

This method is implemented in the ORIGEN code, a well-known and widely spread program for depletion and transmutation calculations. It is used for solving the depletion part of numerous burn-up codes such as MONTEBURNS and MOCUP.

At first sight, the exponential e^{At} can be calculated directly truncating the Taylor series, taking into consideration that the closer to the origin the approximation is, the more accurate the result is. This limitation makes the method unsuitable to solve burn-up calculation where the norm $\|At\|$ is arbitrarily large. Therefore, one technique to improve the accuracy of the series is the scaling and squaring method [20], based on the identity

$$e^{At} = \left(e^{\frac{A}{m}t} \right)^m \tag{15}$$

where m is a power of two, $m = 2^k$, such that the norm $\|A/m\|$ becomes sufficiently small. Verified this condition, the truncated series is calculated for the scaled matrix and the result is squared by repeated multiplications.

This series method with scaling and squaring is implemented in ORIGEN-2.2. Truncations and round-off errors applied to the exponential method solution clearly limit the accuracy of the series expansion. Moreover, the accuracy of the technique can be compromised if the elements of the exponential e^{At} grow as t increases, before they decay, creating a sort of “hump”. Numerical problems appear when this event comes about between t/m and t [21]. Numerical stability and convergence problems, usually encountered using the power series due to the stiffness of the system, are avoided by ORIGEN-2.2 by assuming that the short-lived nuclides decay instantaneously and removing them from the system. They are treated separately by Gauss-Seidel iterative technique [22] under assumption of secular equilibrium of decay and production chains.

2.5.2 Krylov Subspace Approach

The Krylov subspace algorithm has been extensively used and lately it was also applied to burn-up calculations, like in the AEGIS code [23]. It is based on the projection of the original large and sparse matrix *A* to a lower-dimensional Krylov subspace, then the matrix exponential is calculated using the series method or the so-called Padé approximation [24]. This approach determines better approximations of the eigenvalues located in the outermost part of the spectrum of the coefficients, that are those related to the short-lived nuclide that generate problems in most algorithms.
However, it has been discovered that the eigenvalues of the depletion matrix tend to gather along a specific region; therefore different approaches have been implemented to solve burn-up problems, like the Chebyshev Rational Approximation Method (CRAM).

2.5.3 TTA

An alternative method for solving the system of depletion equations is the Transmutation Trajectory Analysis method (TTA) [25], also known as the linear chain method. This is one of the two different options for solving the transmutation and decay equations implemented on the Finnish Monte-Carlo burn-up code SERPENT, based on linearised transmutation chains that can be solved analytically.
The method implies the resolution of the complex web of transmutation reactions and decay, described in the matrix of the coefficients, into a set of linear sub-chains where all possible trajectories and routes through the web are reported. Each sub-channel starts from one single nuclide and follows all possible evolutions it may undergo. The procedure is implemented for every nuclide initially present in the calculation, assuming that they had a non-zero initial concentration, whereas all the encountered isotopes throughout the depletion had a null initial composition. Hence, the superimposition of the obtained results gives the solution of the original problem.
This method can become very complicated whether the reaction modes involved in the calculation increase too much. It is the case of a nuclear reactor: in a transmutations-rich environment, such that a reactor is, to consider all the trajectories is unimaginable. However, the majority of trajectories are definitely negligible and therefore the correspondent chains are terminated before the end.

The main advantages of the TTA method are its easiness in implementation and that it can handle the extensive variations in the transmutation and decay coefficients. On the other hand, one of its most significant drawbacks is the impossibility to treat chains that create closed cycles. In these cases, the problem is solved by terminating the trajectories. Besides, if all the chains are followed until a stable nuclide is found, the computational time can easily become unsustainable [26].

2.5.4 CRAM

The second option implemented in the Serpent code is an advanced matrix exponential solution, developed at VTT, called Chebyshev Rational Approximation Method (CRAM) [13]. This technique investigates the eigenvalues of the matrix of the coefficients *A*. The observation highlighted that a high density of eigenvalues clustered around the negative real axis, confining them in a precise region. This method can be, though, explained as a suitable and optimal rational approximation of the exponential on the negative real axis, that is, for the interval $(-\infty,0]$ [27].

The polynomials of the rational function are then decomposed into poles and residues and, if numerator and denominator orders *k* are selected equal and even, in the Chebyshev approximation the poles form conjugate pairs and the imaginary parts drop out. Since there is no particular reason to select a specific value of *k*, the order of the polynomials is chosen to optimise the accuracy versus the computational running time. In the CRAM implementation used in SERPENT the choice was $k=14$, in order to reduce the mean and maximum error without reaching unbearable running times [28]. The CRAM method can be interpreted as the best rational approximation on the negative real axis, and the robustness and accuracy of its solutions to the burn-up system of equations have been demonstrated and shown in combination with a very short computational time.

2.5.5 RADAU5

More precise methods to solve the depletion system of stiff first-order differential equations with constant coefficients have been developed and applied. Two of the most

stimulating are the backward differentiation formulas BDF [29] and the implicit Runge-Kutta (IRK) of order 5 with 3 stages. The latter is currently implemented in the general purpose ODE solver RADAU5 [30], installed in the version 2 of the ALEPH code for nuclear depletion applications, and it shows an outstanding accuracy that ORIGEN-2.2 cannot even approach. Implicit Runge-Kutta methods have been known to have a high order of solution accuracy and excellent stability properties in solving stiff ordinary differential equations. Hence, the conclusion is that the matrix exponential method of ORIGEN-2.2 cannot solve concentrations as accurately as RADAU5 does. RADAU5 was incorporated in the new version ALEPH2. Its excellent accuracy is however offset by a computational time cost which strongly depends on the size of the matrix *A* of the effective reaction rates. The comparison of the running time for the same calculations, performed by different solvers, states that the matrix exponential method exhibits a weak dependence on the size of the ODE matrix *A*. Moreover, ORIGEN-2.2 is limited by the number of nuclides held in its decay library; therefore it is used to process only those problems where the involved number of nuclides does not exceed ~1700. In principle, it can treat more nuclides, but then problems of convergence and round-off arise, since the complementary nuclides have very short life-times. The IRK method is competitive with the ORIGEN-2.2 solution in terms of CPU time until the number of nuclide considered is smaller than 500. Afterwards it runs more slowly for the majority of the problems (minutes versus second in comparison with the matrix exponential method), but it shows reasonable performances and excellent stability with systems up to ~4000 equations for all known nuclides. The BDF method, used for instance by the deterministic solver DLSODA [31], has a time response which follows the matrix dimension dependence of RADAU5, but it results to be almost two times slower (Fig. 2).

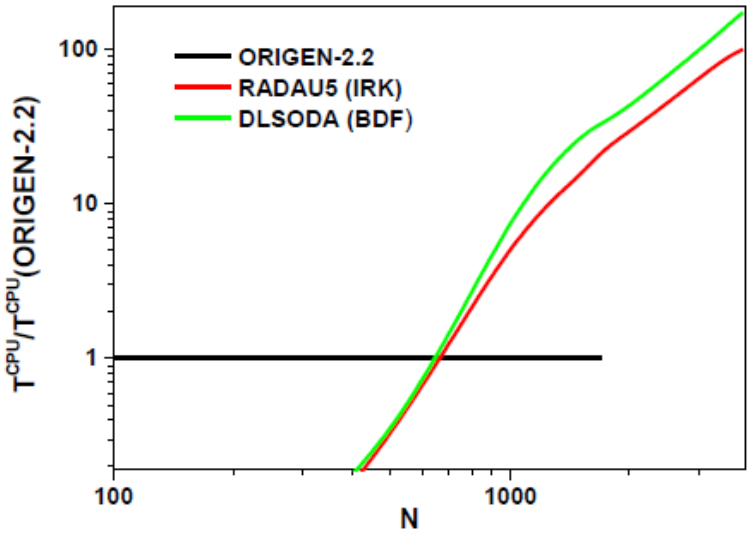

Figure 2: Elapsed CPU time as a function of the number of ODE equations [30].

However, every running time improvement does not influence significantly the total calculation time for typical depletion problems. As a matter of fact, the steady-state Monte-Carlo transport calculation is by far much more time consuming. The CPU required amongst ALEPH modules to complete one burn-up step of the MYRRHA sub-critical core is a good estimator of the fractionation of the calculation time distribution and it is showed in table 1.

Table 1: CPU time share between ALEPH modules to calculate one irradiation step (90 days) of MYRRHA sub-critical core. The MCNP(X) calculations have been performed on 64 CPU cluster under OpenMPI. The number of irradiated materials is 11 (so that reaction rates generator and RADAU5 solver were called 15 times) [30].

	CPU wall time [sec]	*Fraction [%]*
MCNP(X) fluxes and spectra, rsd 0.1%	3.58e+6	99.988
ALEPH generation of average cross sections	19.3	5.4e-4
ALEPH solving ODE by RADAU5	312.5	8.7e-3
(or ALEPH solving ODE by ORIGEN-2.2)	(14.7)	(4.1e-4)
Total		100

The implementation of the RADAU5 solver in ALEPH2 provides a highly accurate isotope inventory at almost invisible, by the user, CPU time share in the whole CPU time elapsed by ALEPH2 run. Besides, the accuracy of the solver makes the nuclear data and

the Monte-Carlo statistical nature, and not the depletion calculation, the two only sources of uncertainties for the nuclide concentrations at the end of the time step.

2.6 Reaction rates analysis

The fundamental feature that determines the feasibility of applying a matrix of the coefficient that evolves linearly in time, as expressed in the system of differential equations $\frac{d}{dt}\vec{N}(t) = A(t)\vec{N}(t)$ with $a_{ij} = a_{0,ij} + b_{ij}t$, is the predictability of the effective reaction rates along the selected period by using a polynomial function. It seems trivial that the reproduction of the irregular evolution of a coefficient, by means of a trend curve that does not adequately fit, will affect the isotopic inventory showing unacceptable results or, at best, a lack of accuracy. Therefore it is essential to analyse the way reaction rates vary during irradiation, in order to define which coefficient may be predicted and which isotopes are more influenced by this technique.

Taking a closer look at the Bateman equation in the formula (1), it is possible to rewrite it in the one-energy-group and spatially average form, assuming that spectra and particle fluxes, as well as cross sections, remain constant in time.

$$\frac{dn_i(t)}{dt} = \sum_{j \neq i} \left[\sum_r \bar{\sigma}_{ji,r}\bar{\phi} + \lambda_{ji}^d \right] n_j(t) - \left[\sum_r \bar{\sigma}_{i,r}\bar{\phi} + \lambda_i^d \right] n_i(t) \qquad (16)$$

After that, reaction rates are gathered with decay constants resulting in two kinds of the so-called effective reaction rates, which are the coefficients of the sparse matrix.

$$\frac{dn_i(t)}{dt} = \sum_j \lambda_{ji}^{tr} n_j(t) - \lambda_i^{tr} n_i(t) \qquad (17)$$

Respectively, the effective reaction rates λ_i^{tr} marked with the subscript *i* are the constituents of the main diagonal, while the parameters λ_{ji}^{tr} correspond to the scattered matrix coefficients that loosely couple the system (Fig. 3).

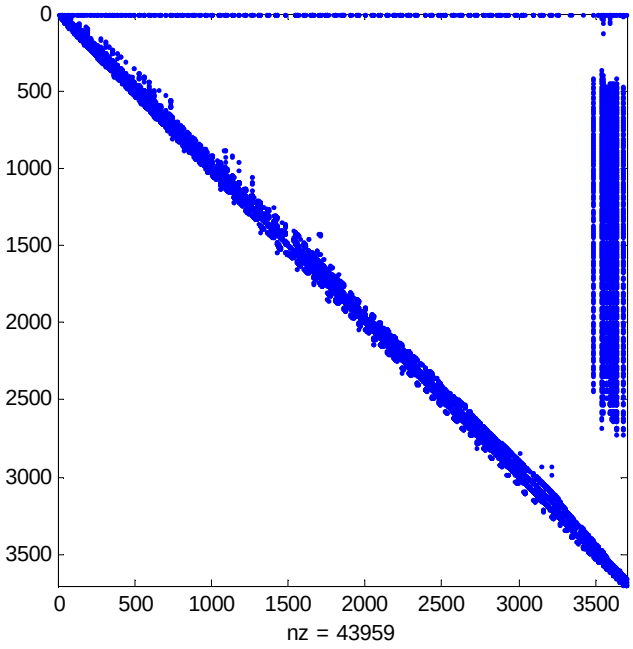

Figure 3: Sparsity pattern of the matrix of the coefficients at the eight irradiation step of the REBUS single-pin model.

The first type of effective reaction rate encloses the single-group energy-averaged transmutation-rates of nuclide *i* from nuclide *j*

$$\lambda_{ji}^{tr} = \lambda_{ji}^{d} + \overline{\sigma}_{j,i}\overline{\phi} \tag{18}$$

whereas λ_i^{tr} represents the one-group energy-averaged disappearance-rate of nuclide *i*

$$\lambda_i^{tr} = \lambda_i^{d} + \sum_r \overline{\sigma}_{i,r}\overline{\phi} \tag{19}$$

which does not give contribution to the coupling of the system.

The disappearance of a specific nuclide subject to an irradiation field takes place following several patterns, collected in the summation and marked with the *r* subscript, that differ from the simple decay mode, if present. ORIGEN-2.2, implemented in the first version of ALEPH, is capable to treat the most of the reactions characteristic of light water nuclear reactors, that is, radiative capture, fission, (n,2n), (n,3n), (n,p) and (n,α).

This is only a limited amount of the possible reaction channels that particles can take in complex nuclear systems – e.g. like ADS problems – with involved energies beyond the standard. In this sense the ALEPH tool has been refurbished in the new version ALEPH2 with the addition of more extensive nuclear data and the RADAU5 solver, able to deal with this increased number of reactions.

Hence, the average cross section $\bar{\sigma}$ in equations (18) and (19) contains contributes of each reaction involved in the problem and it is affected by them. In the depletion calculations processed in this thesis work, neutrons were the only particles involved.

The neutron flux, as well as the total cross section, continuously evolves during the irradiation time: causes of different nature can harden it or make it thermal, therefore affecting both its own and the cross section one-group average value, since the latter is integrally weighted over the flux. The reaction rate $\bar{\sigma}\bar{\phi}$ follows to be the time-dependent part of the effective reaction rate λ^{tr}. On the other hand, the decay rate is by definition constant in time.

2.6.1 Investigative model

The investigation has been carried out into a burn-up credit for a mixed oxide (MOX) fuel [32]. The chosen geometry was a simplified MOX pin cell which related to a typical pin of a17x17 PWR fuel assembly (Fig. 4), that is, cell-pitch and outer and inner radius of the cladding respectively modelled as 1.3127 cm, 0.475 cm and 0.410 cm, as detailed in table 2.

Table 2: Assembly geometry related to a typical 17x17 PWR fuel assembly [32].

Outer radius:	0.475	cm
Inner radius:	0.410	cm
Wall thickness:	0.065	cm
Rod height:	100	cm
Fuel pin pitch:	1.3127	cm

The fuel was a homogeneous mixture of uranium and plutonium oxides placed within the cladding structure. The initial composition for this study represented the range of

potential interest for realistic MOX fuels that would be irradiated in a mixed UO_2-MOX PWR core, alongside UO_2 fuel assemblies with an initial enrichment of 4.3 wt%. The ratio between the total plutonium content and the sum of plutonium and uranium $Pu/(Pu+U)$ was 8 wt%, for a global 5.136 wt% ratio $Pu_{fissile}/(Pu+U)$. A smeared cladding in Zircaloy-2 – a zirconium, iron and chromium alloy – supported the pins to contain the radioactive material. A reduced density has been specified for the fuel pin cladding in order to take into account the presence of the air gap between fuel and cladding. Borated water has been used to moderate and to control the reactivity of the system occupying the remaining empty region of the pin cell. The boron concentration is expressed in table 3. The calculation was performed in a full 3D-geometry with the actual height of the whole system selected to be 100 cm.

Table 3: Non-fissile material data for a typical 17x17 PWR fuel assembly [32].

Cladding:	Zircaloy-2
Coolant/moderator:	Light water, 600 ppm boron

The irradiation history estimated for this benchmark accorded a fixed burn-up time step of 26.25 days for a total amount of 15 irradiation steps. The total power, still fixed, was 1.853398E-02 MW per irradiation step. The number of neutron histories was initially chosen to be 1000 per cycle for 100 cycles, but then changed to 50000 particles per cycle for 200 effective cycles to obtain more precise outcomes.

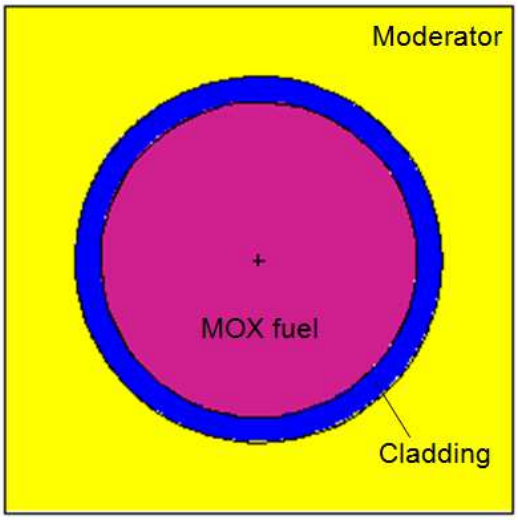

Figure 4: Simplified MOX pin cell.

2.6.2 Results

The first analysis was carried out with the ALEPH2 code using the particle transport Monte-Carlo code MCNPX2.6.0 and the JEFF-3.1.2 nuclear data library. The investigation into the reaction rate evolution only anticipates a vague general trend followed by each matrix coefficient, without furnishing a precise idea of the time behaviour of each rate. Indeed, it is evident from the plot of many selected channels, that a region suitable to be interpolated with a low-order polynomial is far to be found. An example is reported in Fig. 5.

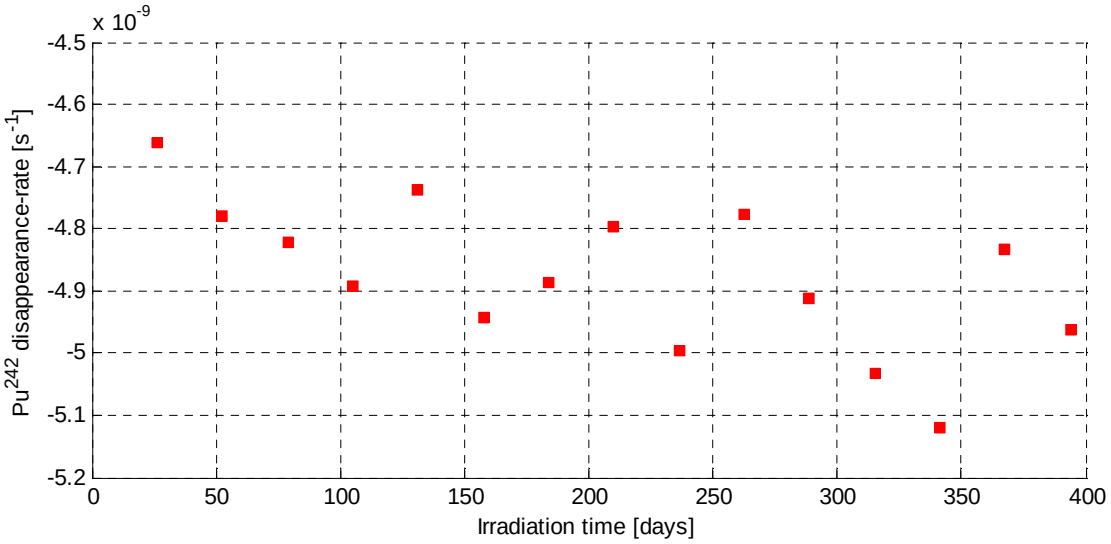

Figure 5: Pu-242 disappearance rate evolution throughout irradiation time for a single-pin model of a typical 17x17 PWR fuel assembly. The MCNP(X) calculation has been performed using 1000 neutron histories per cycle for 100 cycles.

However, amongst the several reactions of the multitude of nuclides described in the matrix, it is possible to distinguish some coefficients that can be already efficiently approximated by a linear function. This is the case of reaction rates of some isotopes like U-235 or U-238, depicted in Fig. 6 and 7.

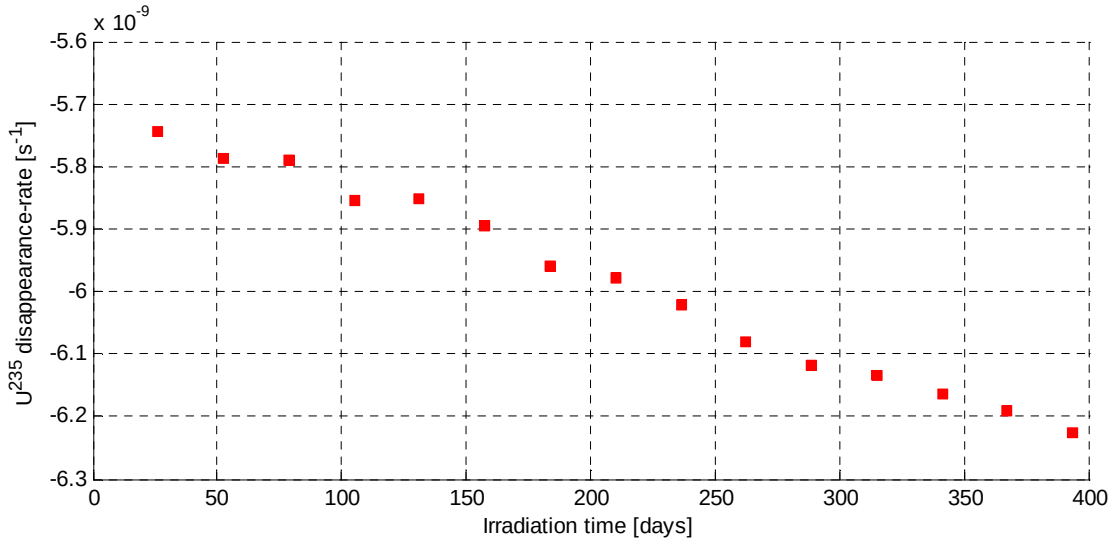

Figure 6: U-235 disappearance rate evolution throughout irradiation time for a single-pin model of a typical 17x17 PWR fuel assembly. The MCNP(X) calculation has been performed using 1000 neutron histories per cycle for 100 cycles.

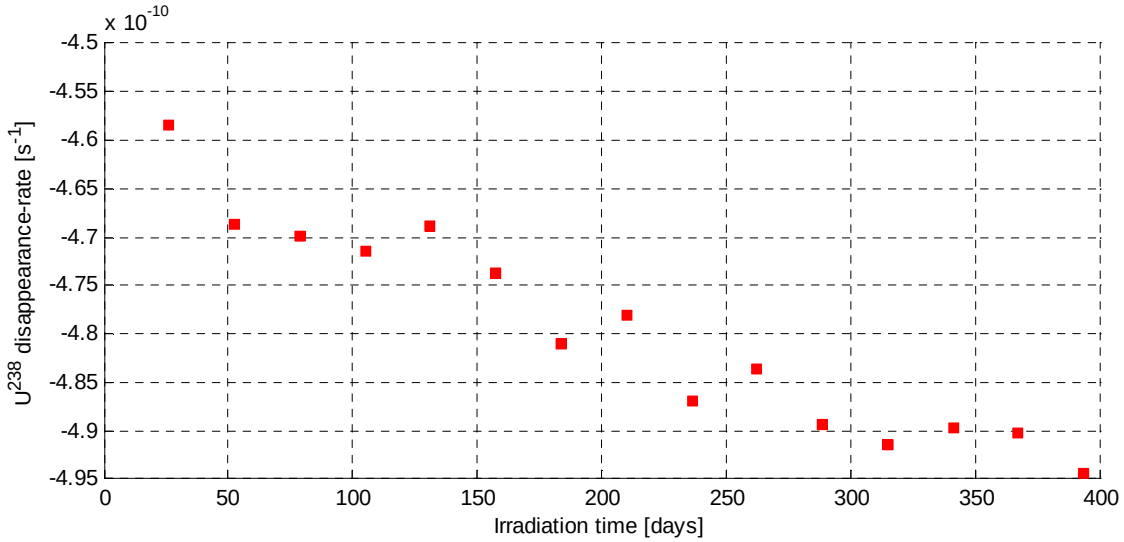

Figure 7: U-238 disappearance rate evolution throughout irradiation time for a single-pin model of a typical 17x17 PWR fuel assembly. The MCNP(X) calculation has been performed using 1000 neutron histories per cycle for 100 cycles.

Other matrix coefficients evolve less regularly. Taking a look at the Pu-242 disappearance reaction rate variation when the material is under irradiation, plotted in Fig. 8, an extremely jerky behaviour is evident.

Focusing on the nature of the matrix coefficients, it is easy to understand that the cause of the scattered trend is the cross section time-evolution, since the decay rate is constant by definition and the flux, in the given conditions, grows regularly.

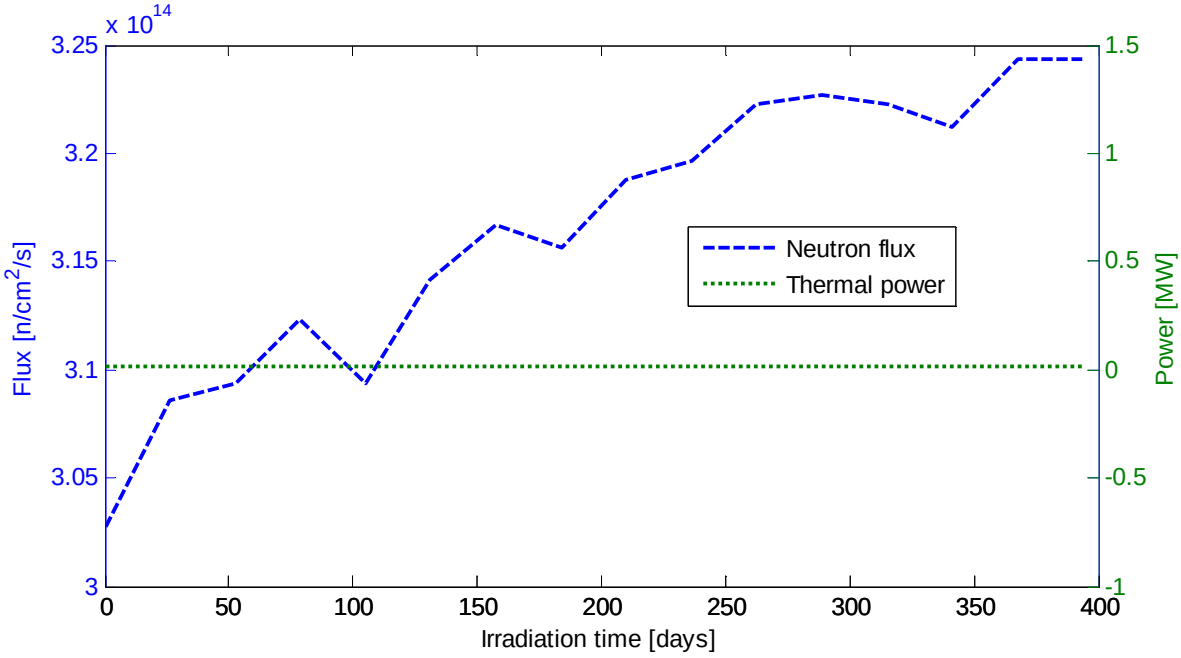

Figure 8: Neutron flux and thermal power evolution throughout irradiation time for a single-pin model of a typical 17x17 PWR fuel assembly.

Checking the given cross section data (Fig. 9), required as ALEPH output at each step, an analogous behaviour is noticed at once. The correspondent total cross section shows a jagged plot as well, therefore it seems legitimate to focus on the cross sections nature and their calculation procedure to research the origin of the perturbation.

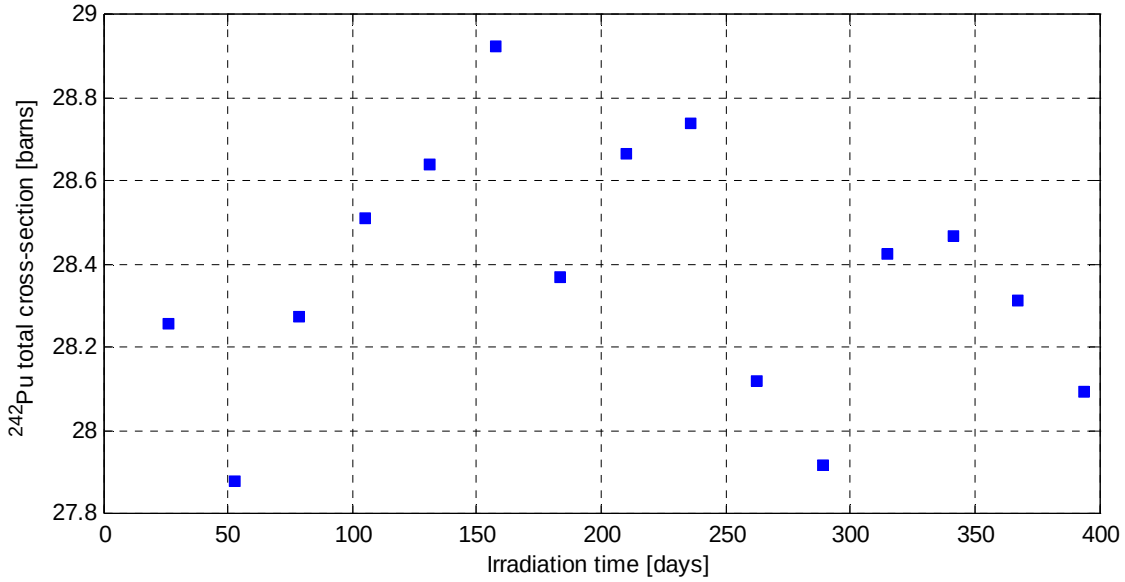

Figure 9: Pu-242 total cross section evolution throughout irradiation time for a single-pin model of a typical 17x17 PWR fuel assembly. The MCNP(X) calculation has been performed using 1000 neutron histories per cycle for 100 cycles.

Although cross sections vary irregularly throughout irradiation, sometimes their evolution does not play a role in the matrix coefficient. The comparison of the reaction rate $\bar{\sigma}\bar{\phi}$ and the decay constant λ^d gives rise to two significant situations:

- If $\lambda^d >> \bar{\sigma}\bar{\phi}$: the decay constant takes over the effective reaction rate, so the progress in time assumes a minor importance on the matrix coefficients construction. This commonly occurs for relatively short half-life elements.

- If $\lambda^d << \bar{\sigma}\bar{\phi}$: the time evolution dictated by the reaction rates is no more negligible. These matrix coefficients are the recommended to be predicted with a time-dependent technique. The nuclides interested by this condition are those which undergo very frequent transmutations and are stable or decay with a long half-life, much longer than ~ $1/\bar{\sigma}\bar{\phi}$.

Nuclides appertained to the first case present extremely short decay-times, sometimes with orders of magnitude of a few seconds or even shorter. The ALEPH code, even if it owns the capability to treat the transmutation rates of these isotopes, does not handle them. Only the decay is considered in the depletion matrix, because of the absence of reaction cross section data for these nuclides.
Because of several irregularity occurrences, it has been retained necessary and more appropriated to proceed with the analysis using higher statistics, in details 11.5 millions of neutron histories: 50000 histories per cycle for 200 effective cycles and 30 to skip. The increase of the number of cycles and neutrons per cycle does not significantly influence the k_{eff} and the total flux because they rapidly converge, but allows to improve the neutron spectrum. In addition, focusing on the very first steps of any reaction rate, it is noticeable that coefficients tend to depart from their general behaviour. For this reason, the irradiation history has been changed, reducing the burn-up interval in the first 78 days to provide a more accurate overview of the phenomenon (Fig. 10).

```
c Irradiation history
IRP t 1.853398E-02 h 6
IRP t 1.853398E-02 h 6
IRP t 1.853398E-02 h 12
IRP t 1.853398E-02 d 1

…
```

```
IRP t 1.853398E-02 d 26.25
IRP t 1.853398E-02 d 26.25
```

Figure 10: Irradiation history of the ALEPH burn-up calculation for a single-pin model of a typical 17x17 PWR fuel assembly. Shorter intervals (6h, 6h, 12h, 1d,…) have been used for the first irradiation steps, whereas they are increased (up to 26.25d) as the irradiation goes by.

`IRP` is an ALEPH keyword used to specify a substep of constant power irradiation, along with the irradiation time: `IRP IRP_option TU TIME`.

`IRP_option` is the power normalisation option – `t` is the shorthand specification for the total power (in MW) – while `TU` is the time unit to be used (d=days, h=hours) and `TIME` is the total time elapsed at the end of the substep since the beginning of the step **[10]**.

The higher number of histories in the calculation traced the tricky coefficients back to an "almost linear" condition. The presence of irregular peaks and the jagged evolutions previously registered drops out both in the cross sections than in the effective reaction rates (Fig. 11 and 12). Hence, it can be inferred that the irregular behaviour has not a physical nature and can be overcome by improving the statistics, rendering the matrix coefficients predictable by using low-order polynomial. The cause that some coefficients have a higher or lower evidence of this occurrence within their neutronic parameters is determined by the amount of data memorized in the JEFF-3.1.2 library – a higher number of data corresponds to a higher accuracy, and vice-versa.

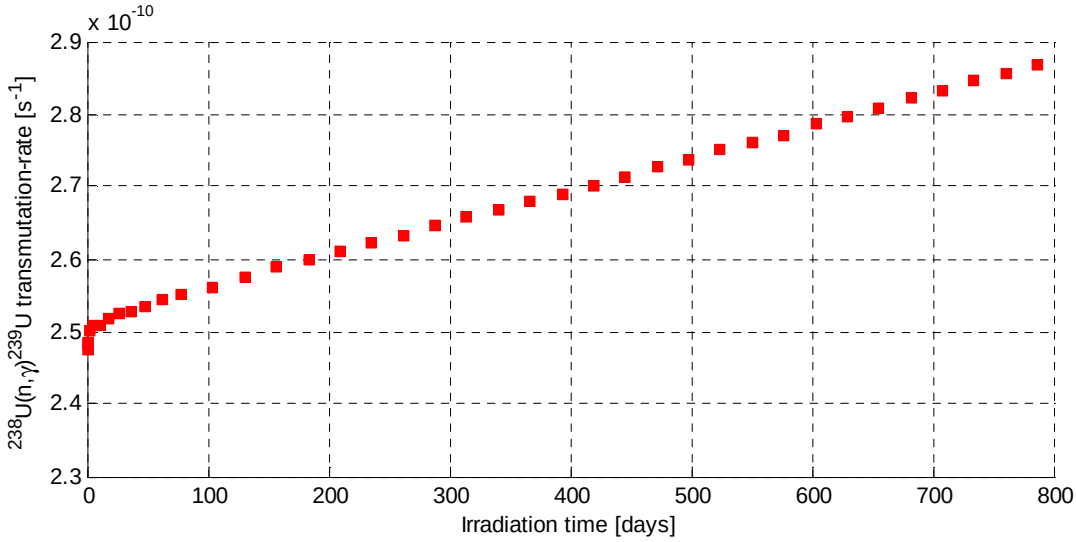

Figure 11: U-238 radiative capture rate evolution throughout irradiation time for a single-pin model of a typical 17x17 PWR fuel assembly. The MCNP(X) calculation has been performed using 50000 neutron histories per cycle for 230 cycles.

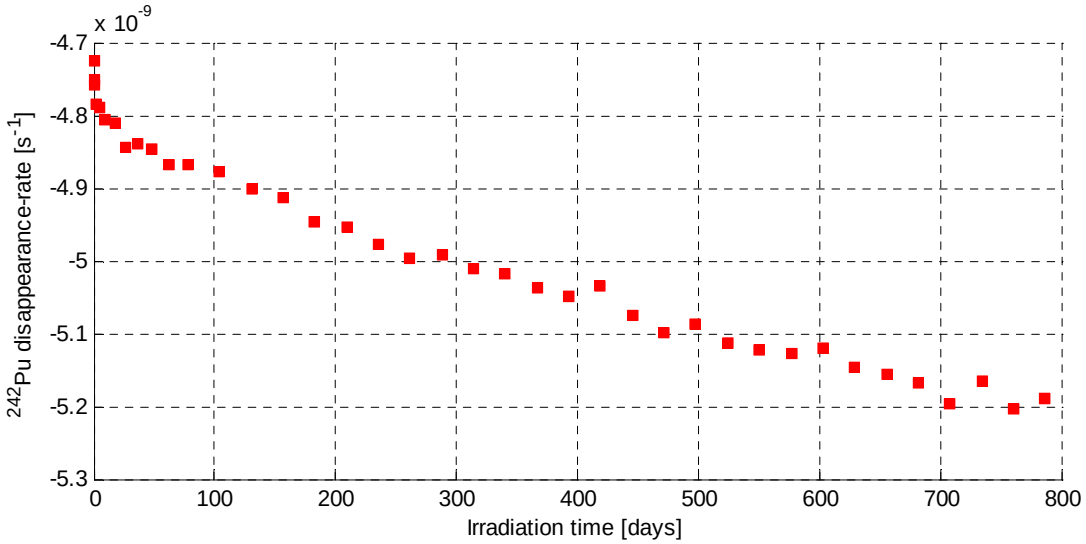

Figure 12: Pu-242 disappearance rate evolution throughout irradiation time for a single-pin model of a typical 17x17 PWR fuel assembly. The MCNP(X) calculation has been performed using 50000 neutron histories per cycle for 230 cycles.

Fig. 11 and 12 highlight a sort of transition period within the very first time steps, where coefficients evolve until they reach a regular behaviour. Moreover, it seems that this transient conditions group together similar nuclides that show the same approaches to their respectively specific trend. Fissile nuclides, fissionable nuclides, main fission products with extremely high absorption cross sections develop along the transient correspondingly comparable behaviours within the same assortment. The sketches of the different reaction rates analysed for this model are reported enclosed in the appendix.

To conclude, from the accurate and thorough investigation into matrix coefficients correspondent to the most relevant nuclides for a burn-up problem, obtained by proceeding a full ALEPH calculation on the PWR single-pin model, it has been observed a general trend throughout the irradiation history that can be easily predicted using a polynomial function. In addition, it can be observed and proved that a linear function fits accurately enough the coefficient changes, provided that the interval undergoing interpolation is not “too long”. The suitable length of the interval has been not well-specified and depends on the studied model, however it was retained acceptable, in order to not extremely reduce the accuracy of the results, to apply the linear interpolation for a maximum of four consecutive steps. In case the user desires to interpolate matrix coefficients for longer intervals, it is suggested to use higher order polynomials or to increase the statistics in the Monte-Carlo computational part.

2.7 Innovative techniques

2.7.1 Predictor-corrector algorithm

In the current ALEPH implementation, matrix coefficients are calculated at the beginning of every time step. The assumption of a constant matrix *A* works well whether the length of the time step is small enough, but sometimes the user cannot or wish not, in order to save computation time, split his time step into several smaller sub-steps. So far, the general practice was to apply predictor-corrector algorithms. This technique guarantees two types of approach: the first concerns fixed time steps, wherein the predictor-corrector method enhances the computational accuracy. As a drawback, the algorithm slows the code because of the continuous MCNP(X) calls, even in intermediate steps. A second methodology aims at increasing the time step length by retrieving intermediate effective reaction rates throughout the irradiation period. It suits particularly well those calculations where the accuracy is fixed, therefore the predictor-corrector will allow the user to reduce the total number of burn-up steps for the full irradiation history simulation. The basic scheme for this approach is shown in Fig. 13:

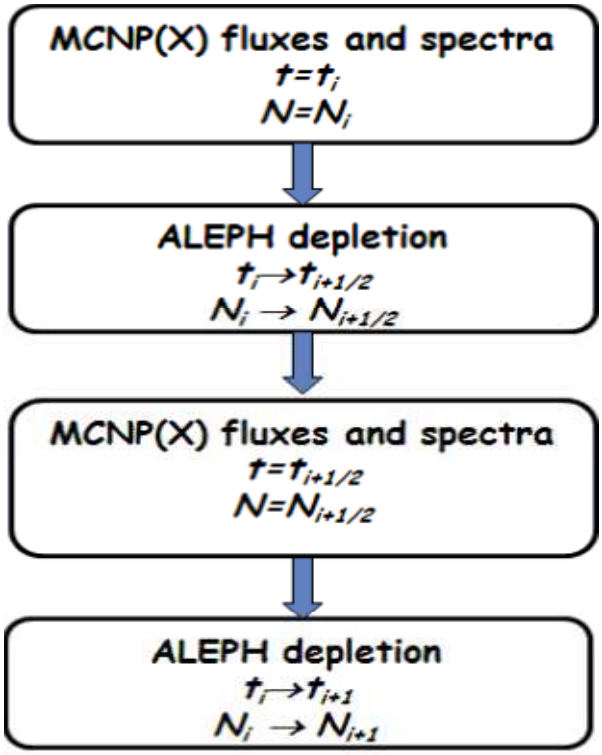

Figure 13: Predictor-corrector algorithm applied in ALEPH 2.1 [10].

The previous version of ALEPH was not programmed to use the predictor-corrector mechanism. In the new edition, in order not to overburden the computational memory, the number of Monte-Carlo calculations per step is reduced to two. Denoting the beginning-of-step time t_i, and the end-of-step time t_{i+1}, the predictor-corrector sequence is interpreted as it follows. First the MCNP(X) code calculates the neutron fluxes and spectra at time t_i, on the basis of the respective nuclide concentrations N_i. Subsequently, ALEPH depletes the isotope densities to half of the step $t_{i+1/2}$, predicting the analogous inventory $N_{i+1/2}$. Afterwards, using the new concentrations, MCNP(X) is launched again and spectra and fluxes at the intermediate step are calculated. These nuclear parameters are, though, collapsed in another matrix of the coefficients and eventually a second depletion calculation is carried out to correct the nuclide densities and obtain N_{i+1} at the end of the step t_{i+1}.

The application of the predictor-corrector method severely increments the running time since it doubles the number of MCNP(X) jobs, thereby in ALEPH2 it has been given the user the possibility whether to apply it or not.

2.7.2 Substep method

The ALEPH code retrieves the effective reaction rates at the beginning of each time step by a Monte-Carlo stochastic calculation. This is usually the most time consuming step of the whole calculation, since it is performed in the real 3D geometry by means of the Monte-Carlo code. Other institutes have already treated computational time consumption issues pouring their energies into increasing the burn-up step, while avoiding any loss of efficiency. Isotalo and Aarnio [33] presented results for different substeps methods for burn-up calculations with Bateman solutions. Their approach consisted in a multi-step approximation based on two assumptions in the time discretisation: firstly the neutronics were solved for a finite number of constant material compositions, that is, cross sections and spectra evolutions were predicted using nuclide concentrations that were constant in time and that referred to specific steady-state solutions. Secondly, they considered a matrix of the coefficients that was constant in time during each burn-up interval. Thus,

since the depletion equation was supposed applicable only with constant coefficients, the neutronic predictions were further approximated using step averages.

Their substep method plans a first neutronic calculation of cross sections and fluxes at the beginning of the step t_0 (BOS). Then, using the parameters calculated at BOS and the neutronics at the beginning of the previous time step t_{-1}, the algorithm predicts time dependent $\sigma(t)$ extrapolated for time spans included between t_0 and t_1, the latter denoted as the end of the step (EOS). The coefficients used to deplete the material are the integral averages of time-dependent neutron spectra and cross sections over the considered span.

$$\sigma = \int_{t_0}^{t_1} \frac{\sigma(t)}{(t_1 - t_0)} dt \qquad (20)$$

The material inventory at the EOS is thereby the input for the new neutronic calculation at the beginning of the step t_1, which predicts the value σ_{pred}. At this stage, if the number of sub-steps is only two, the method stops with the predictor part and starts with the correction, or it goes further on with the successive step according to the request of the user. If the correction of the coefficients takes place, using the neutronics at BOS and the predicted σ_{pred} for EOS, the corrector algorithm re-predicts $\sigma(t)$ for the same interval $[t_0, t_1]$. Then, the integration procedure is performed again to deplete the material throughout the step with the new approximated step-averaged cross sections and spectra. Eventually, the new EOS material compositions become initial compositions for the subsequent burn-up interval. The symbols σ's in this paragraph indicate the required one-group cross sections, neutron fluxes and spectra and whatever neutronic quantity calculated in the steady-state part, that is requested in the depletion calculation.

The substep method reduces to the single predictor approach in case the calculation stops after the σ_{pred} computation: this way halves the computational cost because requires the half of the neutronic calculations, but it also reduces the accuracy; therefore the burn-up step cannot be enlarged.

The use of average values is necessary since the Bateman equation requires, by hypothesis, constant reaction rates. The integrals were calculated numerically as sums of stepwise values: in any case, the effort required by the integration is irrelevant

computationally speaking, as the weight of coefficients are independent of the occurring nuclear reaction and of the nuclide in question, therefore they have to be calculated only once per substep.

To summarise, this method allows to solve the evolution of the isotopic inventory subject to irradiation using piecewise constant coefficients of the Bateman set of equations, rather than constant.

The substep method was tested with six predictor-corrector combinations of substeps over two assembly test cases: a Westinghouse 17x17 PWR assembly with 16 gadolinium-bearing poison rods and a baseline Seed Blanket Unit (SBU) Radkowsky thorium fuel design [34]. The implementation of the technique was utilised on the Monte-Carlo reactor physics code SERPENT 1.1.3 [35]. The test used the library of evaluated nuclear data JEFF-3.1 [36] and three millions neutrons per step. The material depletion was done with the built-in CRAM algorithm of SERPENT.

The combinations of predictor-corrector modules that have been tested, along with their abbreviations, are catalogued in table 4.

Table 4: Predictor-corrector combinations and abbreviations used for them [33].

Abbreviation	*Predictor type*	*Corrector type*
CE	Constant	-
LE	Linear	-
CE/LI	Constant	Linear
CE/QI	Constant	Quadratic
LE/LI	Linear	Linear
LE/QI	Linear	Quadratic

Results were presented by Isotalo and Aarnio [33] for the only CE/LI predictor-corrector method and the two best-performing LE/LI and LE/QI methods.

Using substeps increased drastically the accuracy of the results for short-lived nuclides. Substeps affected to an extent also various non-short-lived heavy metals like U-235 and some plutonium isotopes, since to have a significant effect, the effective half-life of a nuclide only needs to be of the same order of the step length. The use of substeps with the LI/LE method reduced the accuracy of Gd, U-235 and long-lived fission products. This drawback was small, compared to the improvements for the other nuclides, but still highlighted the problematic behaviour that arises from the LE/LI combination relying on

cancellation of errors. Anyway, higher order predictor-corrector combinations did not show this effect and the contribution of substeps resulted only in positive outcomes.

Isotalo and Aarnio came to the conclusion that the quadratic corrector should be the default choice when using the linear interpolation as predictor. Moreover, in order to get better results, the advice was to apply substeps in combination with higher-order predictors and correctors. As a matter of fact, the largest improvement obtained using higher order methods occurred on those nuclides weakly affected by substeps – e.g. like initial gadolinium. On the other hand, the predictor-corrector order had a small effect on short-lived nuclides, where sub-steps provided the largest improvement. Results given by the Aalto University showed that the combination of sub-steps and higher-order predictors and correctors reduces the error on the outcomes of more than a factor of two for essentially all considered nuclides. Alternatively, they give the possibility to enlarge the time span length up to twice the step used without reducing the accuracy and even improving it.

2.7.3 Time-dependent matrix method (TDM)

A unique and innovative feature of depletion codes is the possibility of using time dependent matrix coefficients when solving the system of ODE's. This new implementation is currently in the test phase on the ALEPH2 burn-up code in the SCK•CEN nuclear research centre in Belgium.

As previously stated in the previous sections, the choice of a constant matrix is reasonable only under the assumption of short enough time steps. This condition limits the possibility of having longer time intervals, in particular whether effective reaction rates undergo big changes. Since in the current ALEPH version the neutronic parameters are only calculated by Monte-Carlo method at the beginning of each time step, during a burn-up history a high demand of continuous and cumbersome MCNP(X) calculations is often required. The goal of this new implementation, as well as this thesis work, is to reduce as much as possible the total number of time-consuming Monte-Carlo calculations. The introduction of time-dependent matrix coefficients allows, to a first order, to skip some of MCNP(X) launches and, at the same time, to increase the accuracy of the results. The procedure to implement the time-dependent matrix method is the

following: in essence, the depletion solver resolves the system of differential equations $\frac{d}{dt}\vec{N}(t) = A(t)\vec{N}(t)$, where N is the vector of nuclide concentrations and A is the generally stiff square matrix of coefficients – that now shows a dependence on time. A first assumption to describe the practice is that the three effective reaction rate matrixes immediately before the working step are already known and their time positions are denoted by t_0 at the beginning, t_{0+dt} at the end and $t_{0+1/2dt}$ in the half of the interval. The time-dependent matrix (TDM) technique interpolates the three known coefficients to obtain a polynomial that fits their evolution. Adopting the computed function, matrix coefficients are extrapolated until the end of the next or further time steps (Fig. 14).

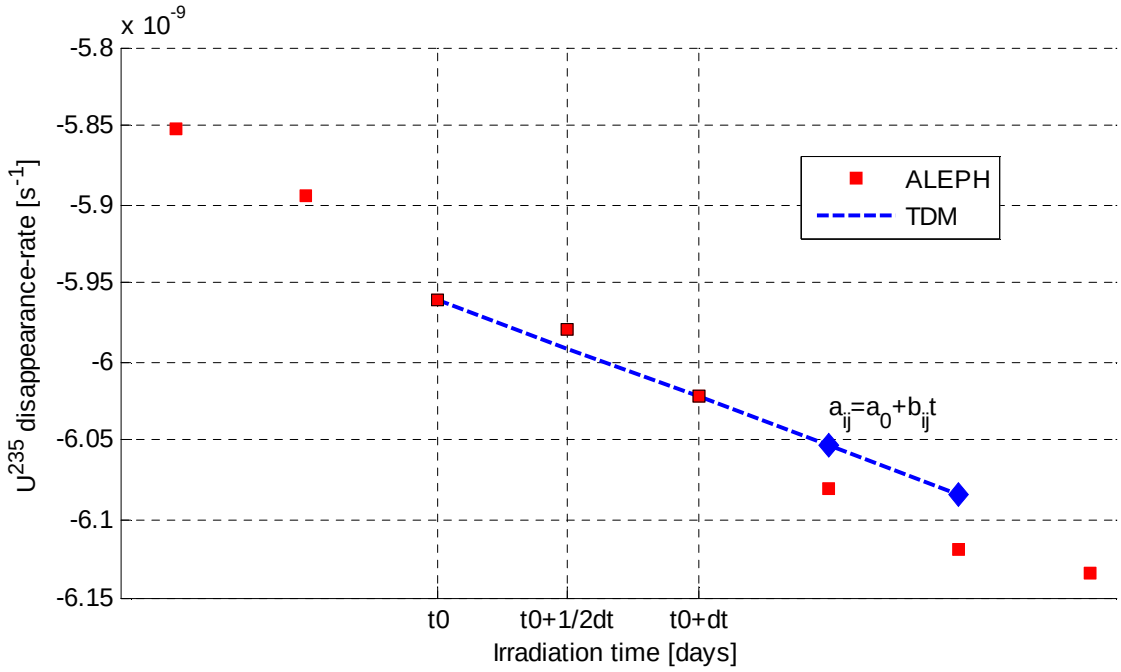

Figure 14: Interpolation and extrapolation process implemented in the TDM method for U-235 disappearance rate for a single-pin model of a typical 17x17 PWR fuel assembly.

In other words, the RADAU5 solver is fed with the function $A(t) = A(0) + f(t)$ instead of using the constant value $A(0)$, as it is usual procedure in the current ALEPH version. The selected and tested extrapolation function of the matrix coefficients has been assessed to be a linear polynomial, therefore the evolution expression becomes $A(t) = A(0) + bt$. This choice does not rule out the potentiality to exploit higher order polynomials, but this option will not be covered within this paper.

The time-dependent matrix method allows to predict the coefficients evolution during irradiation by introducing a numerical algorithm that extrapolates the matrix *A* based upon the analysis of a set of consecutive reaction rate matrixes of time spans immediately ahead. The interpolation of the matrixes sets out the parameters for the extrapolative curve, however the number of steps to interpolate is not fixed. Depending on the chosen function, the polynomial curve gives better results the more it gets closer to the reaction rate trend. If the matrix behaviour proceeds linearly, the use of the TDM technique results highly-suitable; thus the more intimately the real and predicted values match, the higher number of steps can be interpolated.

Implementation of the polynomial technique

The time-dependent matrix of the problem evolves within a single time step, rendering the system of differential equations $\frac{d}{dt}\vec{N}(t) = A\vec{N}(t)$ no more linear in time. In the previous paragraphs it has been stated that extrapolated coefficients of the matrix *A* must follow the polynomial trend $a_{ij} = a_{0,ij} + b_{ij}t$. The investigation starts by interpolating the combinations of reaction rates and decay constants in order to find the coefficients $a_{0,ij}$ and b_{ij} of the linear function. A testing algorithm has been implemented in the ALEPH code to give the user the possibility to make use of the time-dependent matrix method, only by adding an extra parameter to the card describing the irradiation step:

```
p    polynomial_name
```

where `p` indicates the adoption of a polynomial and `polynomial_name` is the name of the selected polynomial data file. This command line is added just after the irradiation specifics for the selected steps and it cannot be used before a decay step, since the TDM does not generate the full required neutronics as MCNP(X) does. The built-in algorithm uses the polynomial function to extrapolate the matrix coefficients throughout the intermediate stages of the selected time interval, providing that the reaction rate at the beginning of the interval corresponds to the reaction rate at the end of the previous step, therefore requiring a shift of the interpolating curve (Fig. 15).

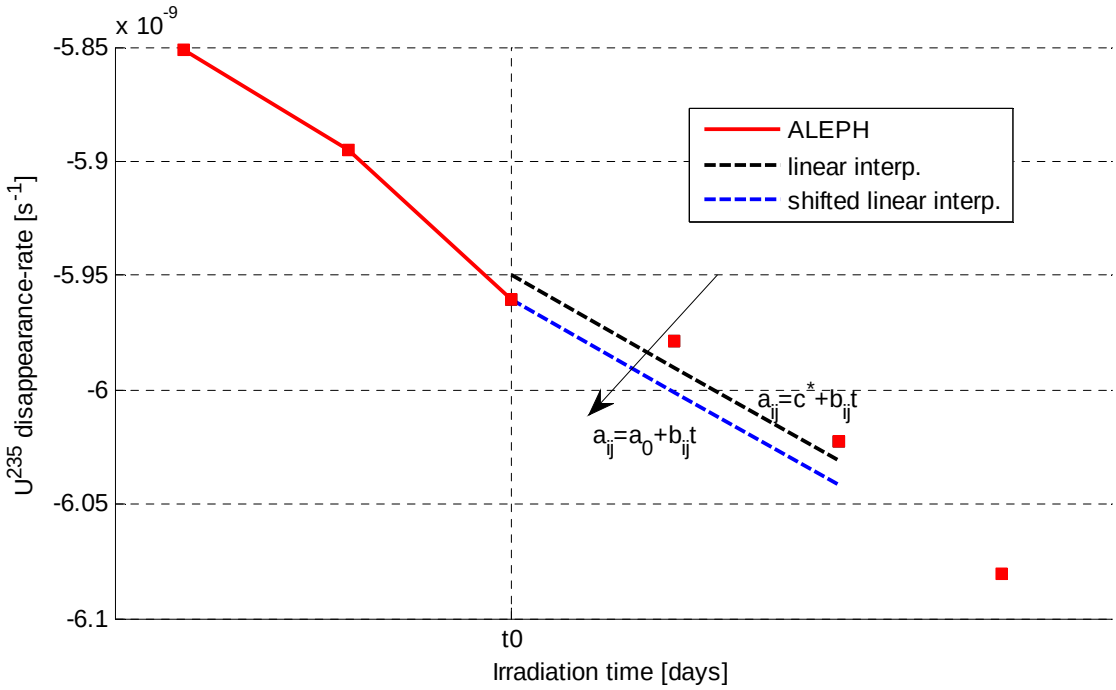

Figure 15: Shifting of the linear interpolating curve implemented in the TDM method for U-235 disappearance rate for a single-pin model of a typical 17x17 PWR fuel assembly.

The parameter $a_{0,ij}$ is the matrix coefficient at the beginning of the processed interval, while b_{ij} is the angular coefficient. These two parameters are calculated for all the nuclides involved in the depletion problem and are catalogued, by means of a built-in MATLAB script, in the polynomial input `.dat` file for as many rows as the number of the isotopes is and along three columns filled in with respectively the two indexes *i* and *j* of the matrix and the ratio of the two coefficients $r_{ij} = \frac{b_{ij}}{a_{0,ij}}$.

```
i          j          ratio_of_the_two_coefficients
```

The choice of submitting a ratio rather than two parameters was motivated by the possibility of applying the technique everywhere within the linear region by only multiplying the ratio *r* by the matrix coefficient correspondent to the chosen time value, since the parameter b_{ij} does not change.

During the test phase, the interpolation was limited relying upon only the list of nuclides for which general purpose neutron-induced nuclear data files are available (as such JEFF-

3.1.2 data library contains files for 380 individual nuclides). Other isotopes gave unstable or incongruent results, probably due to inconsistencies with the numerical solution procedure applied in the RADAU5 solver.

2.8 The REBUS benchmark

In order to assess the accuracy of the innovative time-dependent matrix method, a thorough analysis has been carried out on the REBUS experimental benchmark [37]. REBUS was an international program aimed at providing an experimental database for validation of reactor physics codes used for burn-up credit estimations. The experiment planned the burning of several UO_2 fuel elements, irradiated for four complete cycles in the German commercial PWR at the Neckarwestheim nuclear power plant.

The rods from the fuel assembly from this power plant then underwent first a gamma spectroscopy scan to determine their burn-up profile and later a radiochemical analysis, during which the majority of the radionuclides of interest, in particular to code validation, were determined with high precision. The REBUS experiment considered two different reactors and two different types of fuel, but it was assumed that the uniform nature of the flux in a large commercial power reactor should make simulations relatively straightforward.

The power history had been calculated at the Neckarwestheim NPP applying a licensed deterministic code, for this type of reactors, from the Siemens Company, which used the reactor's thermal output as a normalization factor. A separate computer code was used for the calculation of the fuel and moderator temperature history, whereas the data on the changing boron concentrations over time was available experimentally. The boric acid concentration was therefore kept constant at an average value available in the REBUS report [38]. Moderator, cladding and fuel temperature were kept constant as well.

In the ALEPH model of the power history 54 time steps were adopted, since this was the approach used in the REBUS report and any smaller time step would have overburden the CPU, thereby rendering unbearable the computational time. The 54 steps included 4 batches separated by decay sessions, for a total amount of 50 irradiation and 4 decay periods. Every burn-up time step varied for each interval and the decreasing power underwent step-reductions after every cycle (Fig. 16).

The burn-up intervals were optimised to 30 days for 8 steps within the core of each batch. Shorter steps of 6 and 24 days were selected at the beginning of every irradiation period – after the decay – to better describe the step-variation of power. The decay time spans were respectively of 22, 17 and 15 days, between two consecutive irradiation steps, and 2488 days after the last. Eventually, before every decay step, the last two burn-up intervals were tailored in such a way to get suitable results.

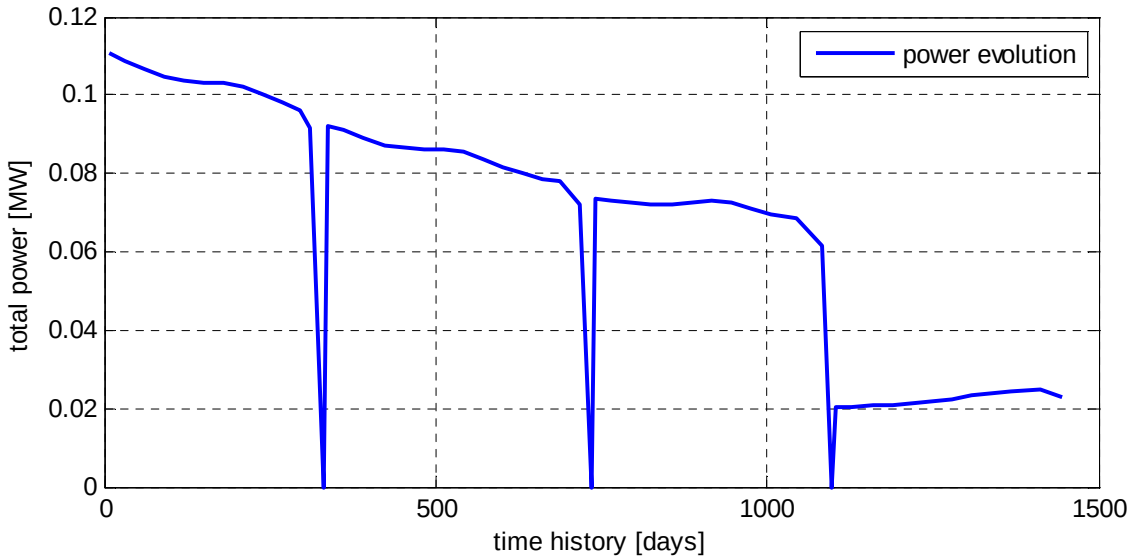

Figure 16: Total power evolution throughout ALEPH irradiation history for the REBUS benchmark.

Concerning the fuel composition, the REBUS report did not specify the percentage of uranium-234 initially present; therefore, assuming that the fuel underwent a process of enrichment by gas diffusion, the composition was later adjusted for the typical presence of the nuclide.

Two different geometries were built: first a single pin and afterwards a ¼ model of the full assembly.

Pin model

Pins have been modeled as approximated 2D structures, since it is a common design for burn-up calculations for PWR's. As a matter of fact, they usually operate so that peaking factors are low and the linear power profile does not change considerably along the axial

direction. The pin model consists of a rectangular prism with a 1.27 cm long pitch, separated in four regions: the outer zone is filled with the moderator which, in turn, embeds the cladding, the gas-filled gap and the inner fuel. The last three regions represent the fuel rod. No division of the pin along the vertical axis was considered. The fuel pellet radius, cladding inner radius and cladding outer radius, measure respectively 4.025, 4.11 and 4.75 mm. The fuel is a homogeneous mixture of uranium oxide UO_2 placed within the cladding structure for a total effective height of 400 cm. A smeared cladding in Zircaloy-2 supports the pins in order to contain the radioactive material. The gap is filled with He to enhance the conductivity and, at the same time, to obtain high-chemical stability with the cladding and the fuel.

Assembly model

The second solution concerns ¼ of the irradiated fuel assembly for a 9x9 square rod configuration. Within the total one quarter of the assembly, three different types of pin were present: standard oxide uranium UO_2 fuel pins, burnable poisons in the form of gadolinium tailored UO_2-Gd_2O_3 pins and empty guide-tube dedicated pins. Amongst all pins, a single one, located in the centre of the assembly, was subject to experimental radiochemical analysis. However, the assembly position in the reactor core was not known and neither was the history of any possible reshuffling. This condition placed restrictions to the performed simulation; therefore the only feasible analysis could be done on the single fuel-assembly than on the full-core level. The nuclides concentrations identified by the radiochemical investigation have been determined with great precision and may be used as a reference. The model has no division of the fuel elements in the vertical direction, but each of the fuel pins was burnt separately – e.g. it was a different material in ALEPH parlance. The power history that has been used is the same reported in Fig. 16.

Eventually, the geometry was modeled, with reflective boundaries on two sides to mimic the symmetry of the system and the white boundaries on the other sides to simulate an infinite assembly array (Fig. 17).

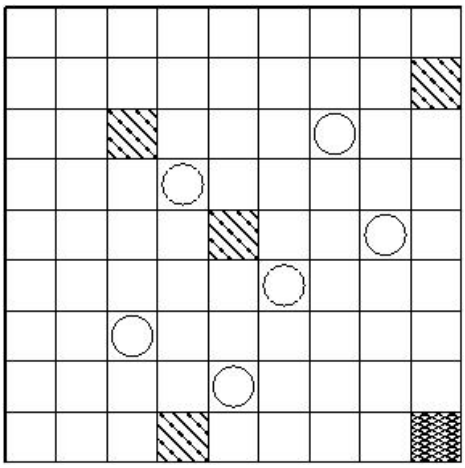

Figure 17: Assembly model. A sketch of the MCNP model of ¼ of the fuel assembly. The heavily shaded pin is the one that was subject to experimental radiochemical analysis. Other UO_2 pins are shown as empty squares. The light shaded pins are Gd-containing rods and the circles represent guide tubes. The heavy-line assembly borders on the left and on the top side depict white boundaries in the MCNP model. The same applies to the axial boundaries. The remaining boundaries were modelled as reflective [30].

2.8.1 Experimental procedure on the REBUS benchmark

Within this thesis work, the depletion evolution simulation with the ALEPH tool has been performed on the single pin model. The test used the general purpose Monte-Carlo radiation transport code MCNPX2.6.0 [7], the JEFF-3.1.2 based nuclear data coupled with the activation data from JEFF-3.1/A and 2000 neutron histories per cycle. The total number of cycles was 250 and the first 50 were skipped. The implemented statistics was chosen to grant an effective reaction rate evolution such that it was possible to pick out polynomial trends throughout the irradiation period. Hence, the first analysis was aimed at identifying the presence of linear regions, if any, throughout the matrix coefficient variation in time.

Four different almost linear regions have been distinguished, wherein the reaction rate trends can be modelled by linear functions of the type $a_{ij} = a_{0,ij} + b_{ij}t$. However, the linearity was not satisfied by all the nuclides involved in the system, therefore the mismatch could become a source of error for the correct processing of the results. Extended investigations have been carried out into the disappearance-rates of the main actinides in the system (U-235, U-238, Pu-239, Pu-240, Pu-241, Pu-242, Am-241, Am-242 metastable, Am-243), as well as into the neutron capture rates (U-235→U-236, U-238→U-239, Pu-238→Pu-239, Pu-240→Pu-241, Pu-241→Pu-242, Pu-242→Pu-243)

and the disappearance of some of the main fission products (Xe-135, Nd-148, Sm-149, Gd-155, Er-167) making good matches with the linear polynomials in the selected interval. Still, the linear interpolation was applied to the list of nuclides described in the previous paragraph. The results were obtained from the direct implementation of the polynomial interpolation method with a MATLAB script. Examples of the disappearance-rate evolution of uranium-235 and uranium-238 are reported in Fig. 18 and 19.

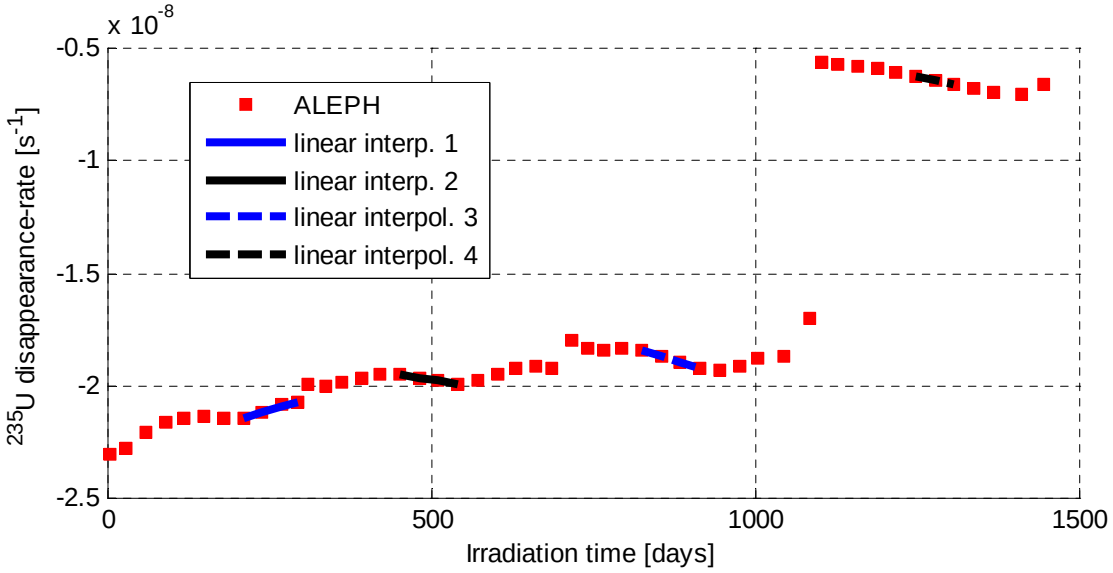

Figure 18: U-235 disappearance rate evolution throughout ALEPH irradiation for the REBUS benchmark. The MCNP(X) calculation has been performed using 2000 neutron histories per cycle for 250 cycles. Within every irradiation batch a linear region has been found.

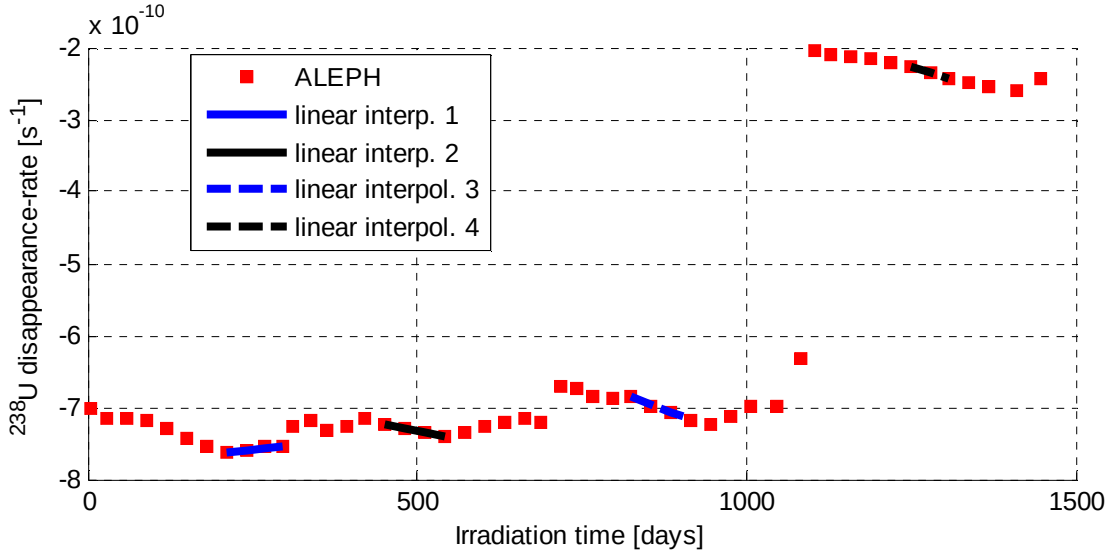

Figure 19: U-238 disappearance rate evolution throughout ALEPH irradiation for the REBUS benchmark. The MCNP(X) calculation has been performed using 2000 neutron histories per cycle for 250 cycles. Within every irradiation batch a linear region has been found.

Time-dependent matrixes have been implemented throughout the four regions, respectively four, four, four and three steps long. The correspondent polynomial data files, namely the `polynomial_1`, `polynomial_2`, `polynomial_3`, `polynomial_4 .dat` files, were then recalled in the ALEPH input script and eventually a full calculation was submitted combining the ALEPH scheme with the innovative feature. Obtained nuclide densities returned in the ALEPH output file after 50 irradiation and 4 decay steps, as well as the isotopic inventory resulted from a combined ALEPH and TDM calculation, have been compared to the nuclide concentrations identified by radiochemical analysis on the experimental test.

2.9 MYRRHA critical core model

The second analysis has been carried out on a model suitable to validate the consistency of using time-dependent matrixes, when the material is subject to a high neutron flux, therefore the MYRRHA critical core configuration has been chosen. The MYRRHA reactor is projected to be the first ADS reactor in Belgium and its construction is dedicated to replace the still operating material testing reactor BR2 in SCK•CEN [16]. An Accelerator Driven System, or ADS, couples a particle accelerator, a spallation target – usually a high atomic mass number metal like lead – which serves as a neutron source and a reactor core. The function of the accelerator is to speed up protons to extremely high energies. Particles then are driven toward the high *Z* spallation target where collide and release a significant number of high-energy source neutrons thanks to the spallation reaction. Produced source neutrons are directed from the spallation target, positioned inside the reactor core, toward the neutron multiplier, where they interact with the fissile material generating fission. The MYRRHA configuration contains a 600 MeV LINAC accelerator, a target material for which lead-bismuth eutectic (LBE) has been chosen and a core of MOX-fuel.

The neutronic 3D model comprises 105 fuel assemblies loaded with 30 at% (Pu, Am) in HM MOX fuel. The core has been subdivided into five zones reflecting the different neutron flux and thus different burn-up levels. The typical BOC (beginning-of-cycle) configuration has been used, which implies that the fresh fuel assemblies are loaded into

the positions close to the core centre, while most burned assemblies (containing already wide list of fission products) are located on the periphery of the core.

The model configuration was completed by seven material testing IPS's, six buoyancy-driven control rods and three CO_2-cooled gravity driven SCRAM rods, LBE-filled box dummy sub-assemblies and dummy assemblies with ZrO_2-Y_2O_3-loaded rods, all enwrapped in the core barrel stainless steel jacket. The geometry and the material data have been taken from available drawings and specifications [39].

The steady-state critical core neutronic calculation was performed using the Monte-Carlo particle transport code MCNPX2.6.0, in combination with the nuclear data library JEFF-3.1.2. The experiment has been simulated carrying out a full ALEPH2 calculation for an equilibrium cycle of 90 days, split in ten spans of 9 days each and terminated by a one day long pure decay session (Fig. 20). The power was kept constant throughout all irradiation steps. Thermal power release and neutron flux are plotted in Fig. 21.

```
c HISTORY  - 1 equilibrium cycle
  IRP t 94.5     d 9.
  IRP t 94.5     d 9.
  IRP t 94.5     d 9.

  …

  IRP t 94.5     d 9.
  IRP t 94.5     d 9.
  DEC            d 1.
```

Figure 20: Irradiation history of the ALEPH burn-up calculation for the MYRRHA critical core configuration.

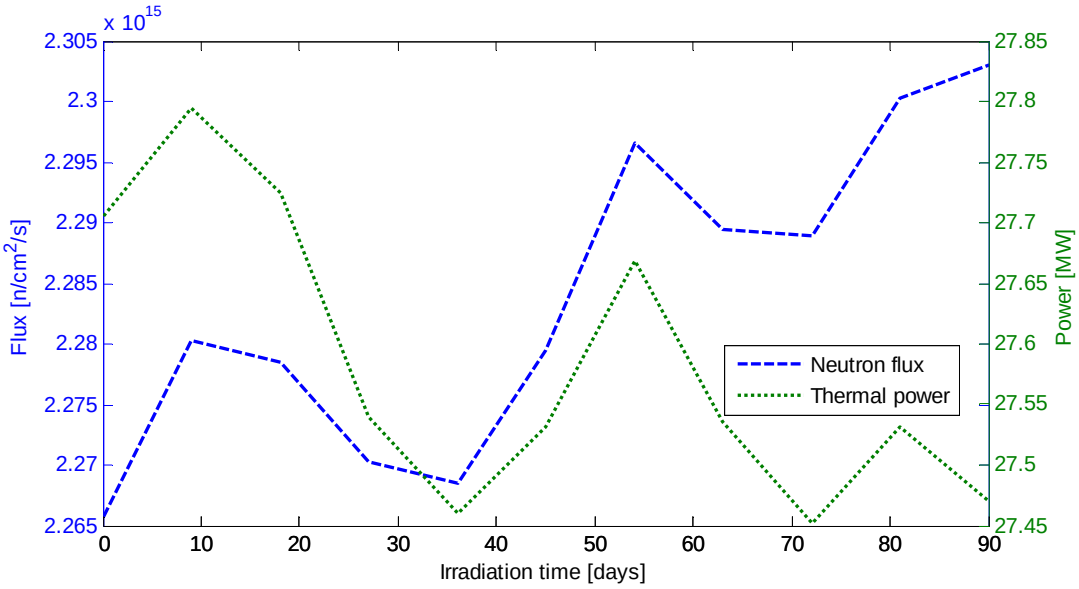

Figure 21: Neutron flux and thermal power evolution throughout 90 days of irradiation for the MYRRHA critical core configuration. Reported thermal power is related to only one group of assemblies, but the total power release remains constant.

Retrieved results were, though, set as reference values for the TDM technique validation. Both the analysis with pure ALEPH and combined with TDM used 10000 nuclear histories per cycle for 150 cycles, skipping the first 50. The time-dependent matrixes were tested in the eighth irradiation single-step before, and two consecutive steps, the eighth and the ninth, after.

The interpolation region has been selected with the same criteria as in the REBUS experiment, being sure that the linearity conditions were fulfilled (Fig. 22 and 23).

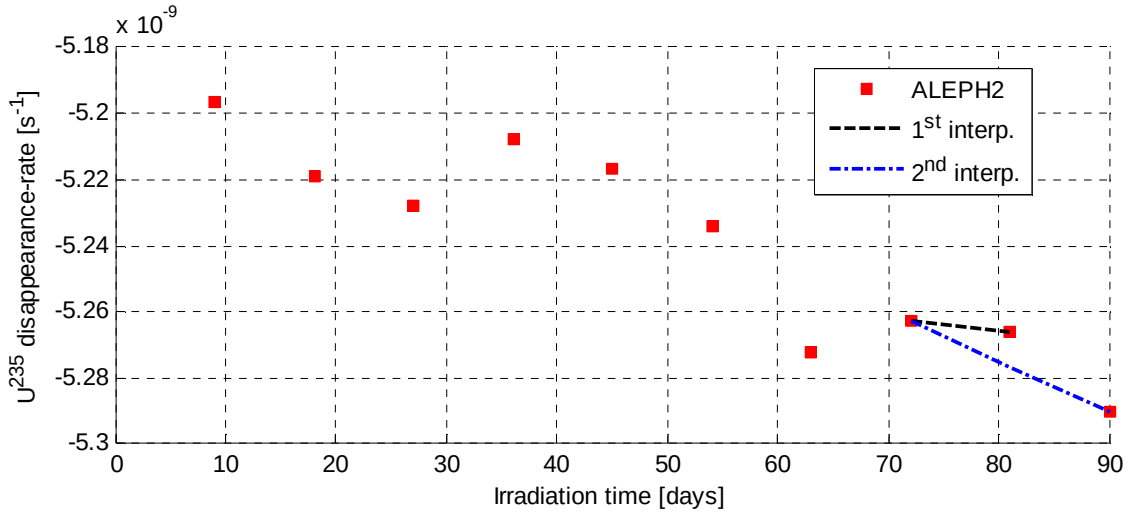

Figure 22: U-235 disappearance rate evolution throughout 90 days of irradiation for the MYRRHA critical core model. The MCNP(X) calculation has been performed using 10000 neutron histories per cycle for 150 cycles. Within the irradiation history, the interpolation was performed both on a single interval and two consecutive intervals.

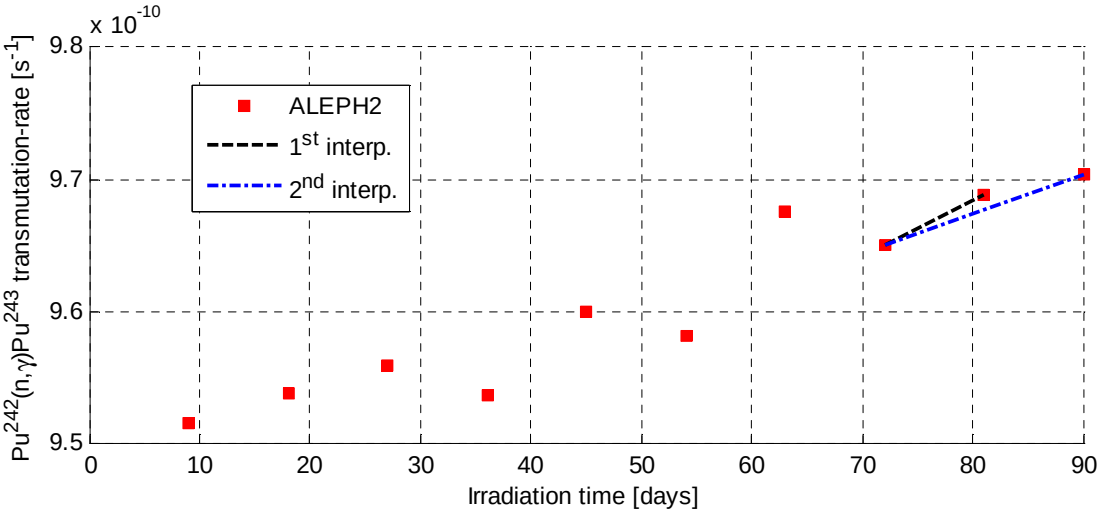

Figure 23: Pu-242 radiative capture rate evolution throughout 90 days of irradiation for the MYRRHA critical core model. The MCNP(X) calculation has been performed using 10000 neutron histories per cycle for 150 cycles. Within the irradiation history, the interpolation was performed both on a single interval and two consecutive intervals.

In addition, an alternative configuration was modelled, in order to extend the validity of the test. The power history was modified, adding a further 90 days long batch of irradiation after 30 days of decay, and concluded with other 30 days of decay session at the end of the burn-up analysis. Again, thermal power and neutron flux are sketched in Fig. 24.

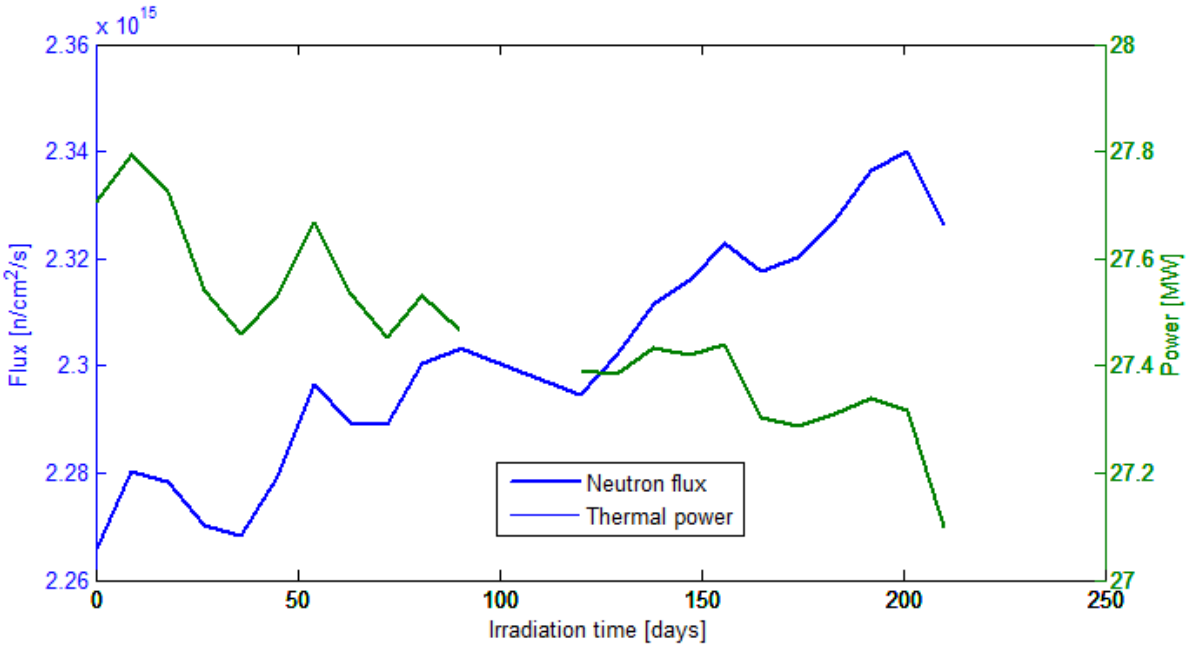

Figure 24: Neutron flux and thermal power evolution, related to one group of assemblies, throughout two batches of irradiation separated by decay for the MYRRHA critical core configuration.

The MCNP statistics was kept the same, while the interpolated intervals in this case were the eighth, the ninth, the nineteenth and the twentieth. The interpolation procedure was the same as already described in this same paper.

Chapter 3

Results and Discussion

3.1 Analysis of the results – REBUS Benchmark

The combination of the TDM technique and ALEPH2 burn-up analysis returned the nuclide concentrations throughout every step of the irradiation history of the REBUS experiment, within the ALEPH output file. The results at the end of the 54th and last step for both the single-pin (Fig. 25) and the assembly model (Fig. 26) were compared with the experimentally determined concentrations. The same procedure has been followed also to inspect the pure ALEPH2 results for the same models, irradiation history and statistics (Fig. 25 and 26). To investigate into the final concentrations, all the nuclide densities have been normalised with regard to the U-238 isotope by calculating the ratio of the concentrations. Eventually the deviations have been retrieved by computing the relative error with respect to the experimental data. The results are given in table 6 and Fig. 25, 26 and 27.

The outcomes may be deemed satisfactory since ALEPH2 and combined ALEPH2 and TDM inventories get very close one another in both the two models. Moreover, the average absolute difference between the experimental and calculated concentrations is 16.4% for ALEPH2 single pin, while using time-dependent matrixes it goes slightly down to 16.3%. For the ¼ assembly it is 14.5% for both ALEPH and TDM.

The most significant variations can be attributed to the main actinides like uranium, plutonium, americium and curium, and more in particular to Cm-242 and Am-242*m* for the pin model, Np-237 and Pu-238 for the assembly. However, although the first two

isotopes generate better outcomes with the TDM technique, the latter bring to a lack of accuracy compared to the genuine ALEPH2 calculation, carrying an overestimation of their densities up to 1.25% higher than the ALEPH predicted results for the single pin.

The ALEPH2 code has been already appreciated in its comparison with the previous version ALEPH1, as claimed by Vidmar, Stankovskiy and Van den Eynde [30] in their SCK•CEN internal work of validation of the ALEPH2 code on the REBUS experimental data, because the discrepancies found with the older version of ALEPH were no longer present. The TDM method gives, for these isotopes, results qualitatively comparable to ALEPH2, therefore also in this analysis the above-mentioned problem can be considered overcome. Eventually, it can be stated that the combined ALEPH2 with TDM single-pin results are very consistent with the pure ALEPH2 ones.

The outstanding feature of this innovative technique is the conspicuous reduction of computational time. Once again, it is important to bear in mind that the time-dependent method avoids the time consumption due to continuous recalling of MCNP(X) calculations at the beginning of every step. Thus, the gain in computational time can be roughly calculated by adding up the time spent in processing the Monte-Carlo part for those intervals suitable for the use of TDM. The ratio between the computational times has been broadly measured to remarkable values – of ~78% for the pin calculation and ~82% for the assembly, that is, the cumulative time spent in the calculation is reduced almost of one quarter.

As far as the accuracy of the method is concerned, its measurement has been calculated over a group of 46 isotopes calculating the root-mean-square deviation (RMSD) and comparing the experimental data firstly with the pure ALEPH2 results and then with the combined ALEPH2 and TDM outcomes. In the measurement, also the standard deviations of the densities obtained by radiochemical analysis in the REBUS experiment have been considered, using the statistical formula

$$RMSD(\hat{n}) = \sqrt{\frac{1}{N}\left(\frac{\hat{n} - n}{\Delta\sigma}\right)^2} \qquad (21)$$

where N is the number of isotopes considered in the analysis, $\hat{n}$ is the calculated concentration for a single nuclide, n is the experimentally measured density of the correspondent nuclide and σ is the standard deviation measured in the experiment. The

calculation shows a slightly higher accuracy by using time-dependent matrixes, as reported in table 5.

Table 5: Statistical accuracy of the REBUS experiment comparing outcomes retrieved with pure ALEPH and combined TDM and ALEPH code.

	RMSDALEPH/RMSDALEPH	*RMSDTDM/RMSDALEPH*
Single-pin model	1	0.976
Assembly model	1	0.987

Combined, the improvement in accuracy and the reduction of computational time, back the time-dependent matrix method as an innovative feature, owing extraordinary characteristics that can, to all intents and purposes, put itself forward amongst one of the main improvement of the next ALEPH version.

3.1.1 Actinides

Also for the mere actinides, the compared accuracies between experimental and calculated isotope concentrations, first with ALEPH2 and after with the TDM method, tip the scales in favour of the latter. Indeed, the average relative error of the actinides involved in the calculation, in the single pin configuration, is 16.61% in the first case and 16.39% in the second. Amongst them, uranium and almost all plutonium and curium isotopes (Pu-239 and Cu-242 apart), are characterised by errors smaller than the average in both cases. On the other hand neptunium and americium deviations exceed 30%, with peaks up to 39%, this is due to high uncertainty on nuclear data for these isotopes. Anyway, the use of time-dependent matrixes brings to a general increase in accuracy averaged amongst the actinides in both assembly and pin configuration.

The peak of error displayed on the Cm-242 for ALEPH calculations, of the order of 60% for the pin and 50% for the ¼ assembly, is noticeable also in the TDM results, but it is cut ~1% off. The other curium isotopes do not present significant errors, albeit their quantification using the new technique is anyway improved.

3.1.2 Fission products

Fission product outcomes agree with the satisfactory match, already proved during the ALEPH2 testing. As far as the radionuclide concentrations most important from the waste management point of view are concerned, such as Cs-135 and Tc-99, a satisfactory match is noticed. The same comes about for the Cs-137 isotope, which was used for experimental gamma scanning, aimed at burn-up profile determination. The time-dependent matrix method gives optimal results for these nuclides with discrepancies of the order of a few tenths of percent or lower and often counterbalanced, compared to the ALEPH2 concentrations. Same performances are achieved also for cerium, molybdenum, ruthenium, rhodium and silver isotopes in the assembly burn-up calculation, while the pin configuration gives worse outcomes. The results of most Sm and Pd isotopes are disappointing due to poor knowledge of neutron induced fission yields, but the TDM technique contributes to give them an overall better accuracy. Although the samarium shows a trade-off amongst its isotopes deviations, the palladium displays a difference in the relative errors of its isotopes using ALEPH2 and TDM that is 0.11% on average. The lack of accuracy may be attributable to the jagged evolution of the reaction rates throughout the selected interpolated intervals.

3.1.3 Burn-up indicators

Neodymium is a stable fission product with a very low migration within the UO_2 matrix of the fuel, its concentration is therefore an accurate measure of the local or averaged burn-up. The match between the experimental data and the ALEPH2 calculations is very good, resulting in correct burn-up values used in the model. The TDM applied to the assembly model shows a little drawback for these isotopes, deviations are on average 0.2% bigger than the ALEPH2 results, apart for the Nd-143, which has a small improvement (deviation from 3.94% to 3.81%), and the Nd-142, with an error which differs of 0.42%. For the pin model this misbehaviour is generally not occurring. For the current requirements of the nuclear industry, the achieved accuracy obtained in the both ways can be deemed satisfactory.

Table 6: Experiment and calculations. The relative difference in percent between the calculated and the measured normalised values of the concentrations of radionuclides in the sample for the reference date of June 8, 2004. The normalisation was done with regard to the concentration of U-238. The ALEPH2 and the combined TDM and ALEPH2 code were used with the pin and assembly models. The absolute measured concentrations and their uncertainties are listed as well.

	CALCULATIONS				MEASUREMENTS	
Nuclide	**TDM PIN [%]**	**TDM ASSEMBLY [%]**	**ALEPH2 PIN [%]**	**ALEPH2 ASSEMBLY [%]**	**C [mg/g]**	**2s(C) [%]**
U-234	6.5%	6.9%	6.4%	7.2%	0.161	5.0%
U-235	5.5%	4.5%	6.1%	4.8%	5.56	0.7%
U-236	0.0%	0.2%	0.1%	0.2%	5.81	0.7%
U-238	0.0%	0.2%	0.0%	0.2%	1000	0.6%
Np-237	32.6%	29.7%	33.1%	28.6%	0.66	20.0%
Pu-238	6.7%	1.9%	6.5%	0.7%	0.467	3.1%
Pu-239	19.7%	12.9%	20.2%	13.2%	6.26	0.6%
Pu-240	4.7%	2.7%	4.9%	3.4%	3.48	0.6%
Pu-241	13.8%	7.5%	13.7%	7.2%	1.434	0.6%
Pu-242	-1.1%	-2.3%	-1.2%	-2.5%	1.272	0.6%
Am-241	37.5%	29.9%	37.3%	29.5%	0.55	3.7%
Am-242m	38.0%	26.4%	39.0%	27.4%	0.0017	11.0%
Am-243	32.0%	26.6%	31.4%	26.2%	0.27	3.5%
Cm-242	61.7%	48.8%	62.7%	49.8%	0.0000042	36.0%
Cm-243	-3.2%	-9.8%	-3.9%	-9.9%	0.00085	20.0%
Cm-244	0.6%	-6.3%	0.7%	-6.6%	0.146	2.5%
Cm-245	14.9%	-0.5%	15.1%	-0.1%	0.0144	5.6%
Ce-144	-0.3%	-1.6%	0.1%	-1.2%	0.00069	10.0%
Nd-142	-4.9%	-6.6%	-5.4%	-7.0%	0.0566	0.8%
Nd-143	5.6%	3.8%	5.9%	3.9%	1.162	0.6%
Nd-144	0.7%	0.4%	0.5%	0.1%	2.449	0.6%
Nd-145	2.7%	2.4%	2.8%	2.3%	1.081	0.6%
Nd-146	3.5%	2.2%	3.4%	1.9%	1.276	0.6%
Nd-148	4.7%	3.7%	4.7%	3.5%	0.647	0.7%
Nd-150	4.1%	2.8%	4.1%	2.7%	0.32	0.7%
Sm-147	-1.2%	-0.3%	-1.0%	0.0%	0.324	0.8%
Sm-148	13.6%	11.0%	13.6%	10.5%	0.313	0.8%
Sm-149	-88.5%	-89.3%	-88.5%	-89.2%	0.0259	2.1%
Sm-150	-2.9%	-4.3%	-2.8%	-4.5%	0.518	0.8%
Sm-151	13.4%	6.6%	14.3%	7.7%	0.01559	0.9%
Sm-152	-4.6%	-2.5%	-4.3%	-2.7%	0.1589	0.8%
Sm-154	8.8%	6.4%	8.9%	6.4%	0.0727	0.8%
Eu-153	2.5%	1.6%	2.5%	1.6%	0.2086	0.9%
Eu-154	21.1%	14.4%	21.5%	14.5%	0.0256	3.4%
Eu-155	-18.0%	-19.7%	-17.3%	-19.3%	0.007	6.0%
Gd-155	-5.7%	-7.9%	-4.8%	-7.3%	0.0107	5.1%
Cs-133	5.2%	5.0%	5.4%	5.0%	1.74	2.6%
Cs-135	6.2%	3.1%	6.5%	3.1%	0.625	2.6%
Cs-137	0.7%	-0.4%	0.7%	-0.5%	1.83	2.6%
Mo-95	13.8%	13.2%	13.8%	13.0%	1.13	9.9%
Tc-99	-1.7%	-2.2%	-1.6%	-2.2%	1.36	10.0%
Ru-101	33.2%	32.0%	33.2%	31.9%	1.05	9.9%
Rh-103	22.8%	21.6%	23.1%	22.0%	0.63	10.0%
Pd-105	63.8%	60.5%	63.9%	60.5%	0.49	9.8%
Pd-108	68.7%	64.8%	68.9%	64.9%	0.192	9.8%
Ag-109	46.7%	43.5%	46.7%	43.8%	0.116	10.0%

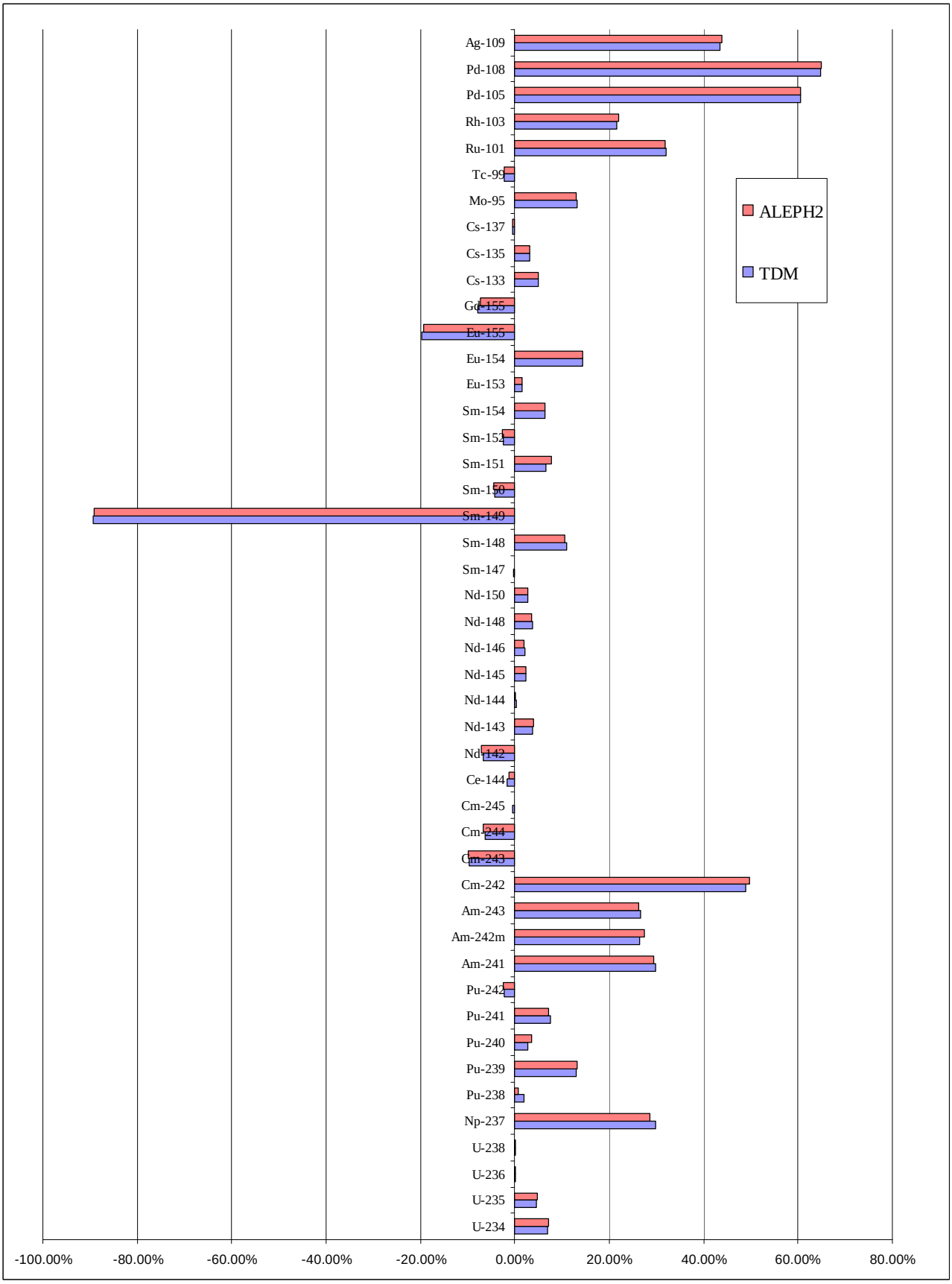

Figure 25: Comparison of ALEPH2 and coupled TDM and ALEPH2 code for the REBUS assembly model. See also table 6.

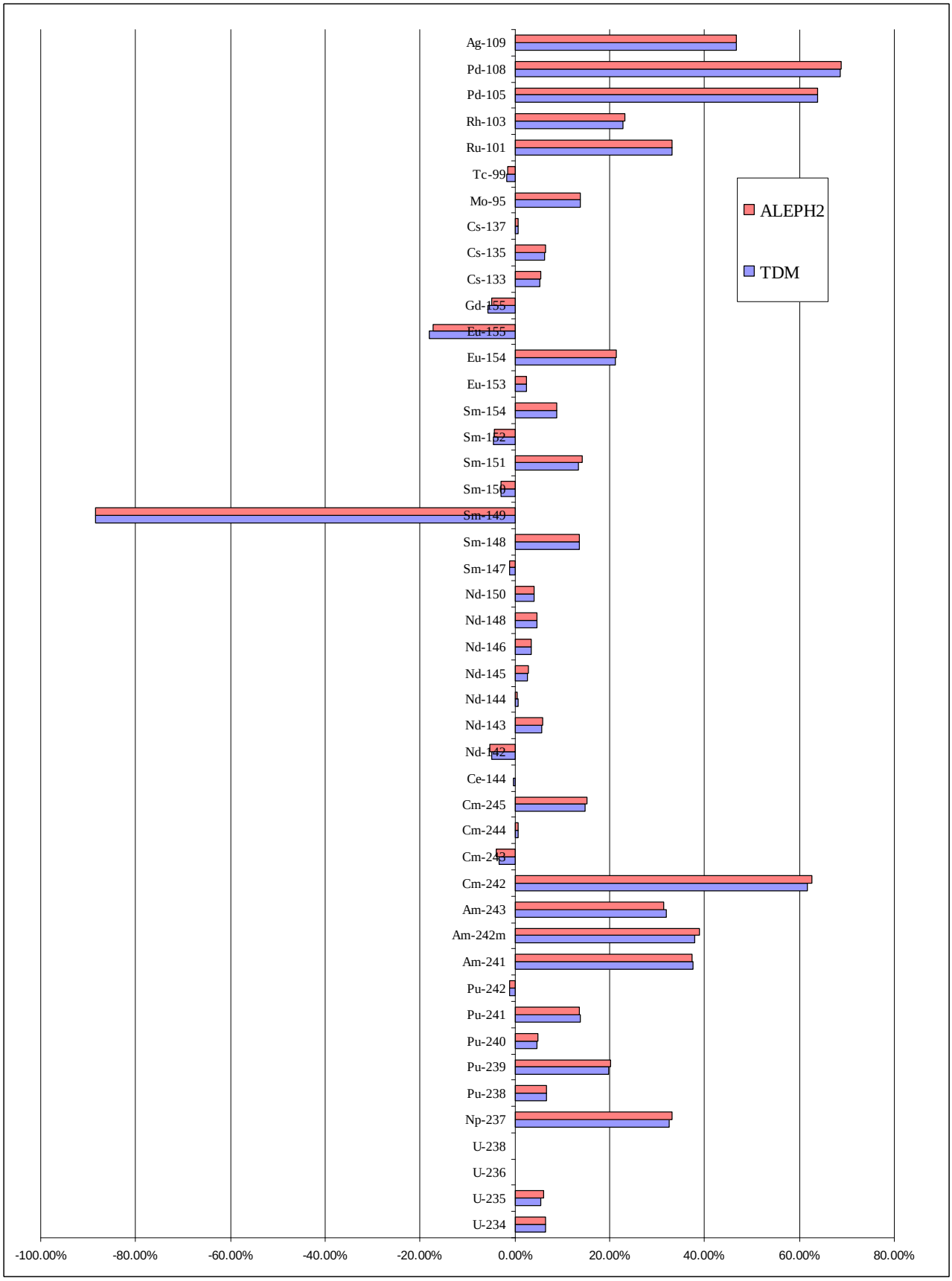

Figure 26: Comparison of ALEPH2 and coupled TDM and ALEPH2 code for the REBUS pin model. See also table 6.

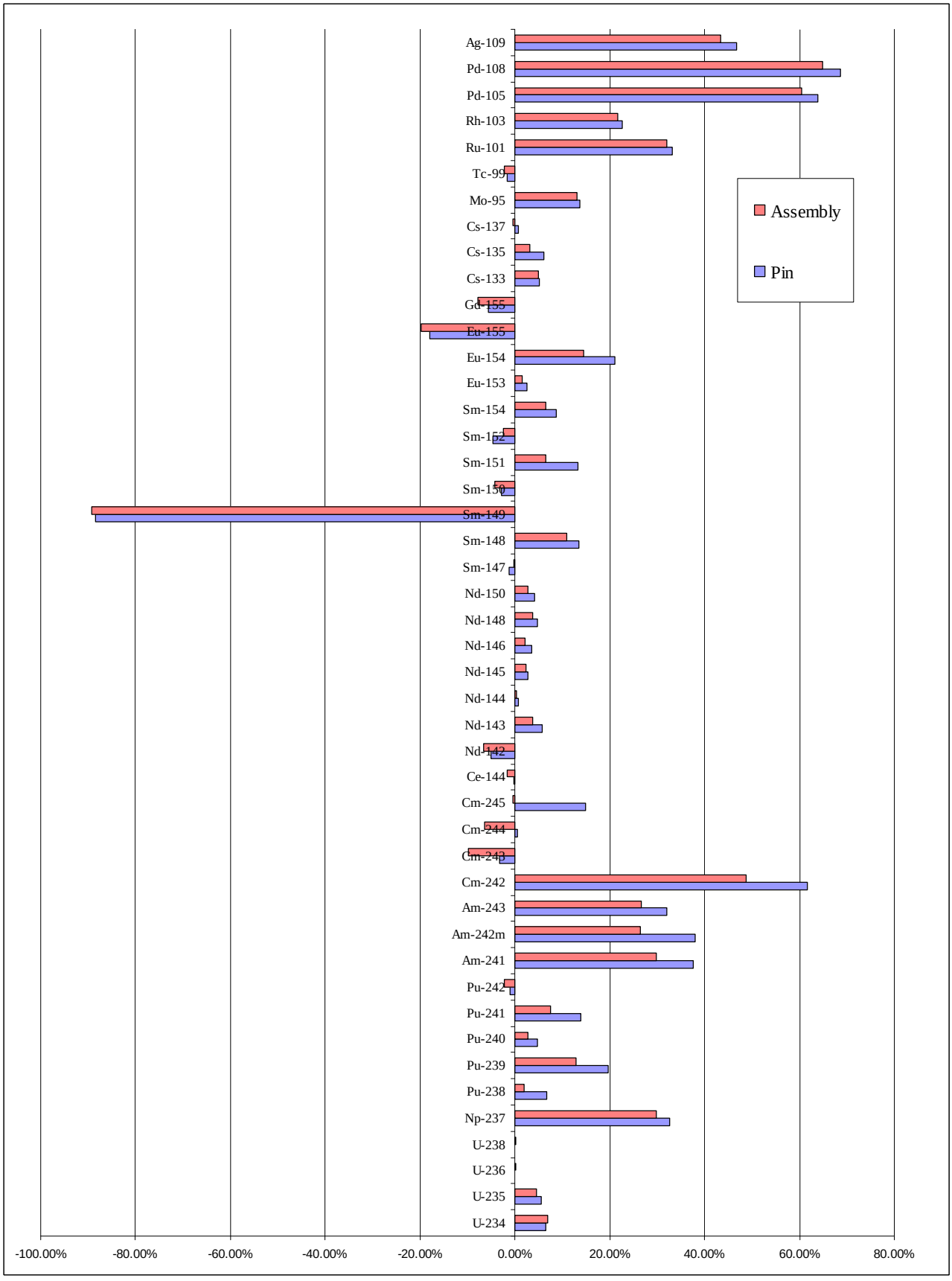

Figure 27: Comparison of the results of TDM technique for the REBUS assembly and pin model. See also table 6.

3.2 Analysis of the results – MYRRHA critical core

Nuclide concentrations at the end of the burn-up calculation, obtained using time-dependent matrixes, were compared to the same inventory retrieved after launching ALEPH2 for the same model and irradiation history. By evaluating a high-flux core configuration the final outcomes are remarkable, extremely close to the ALEPH2 results, backing the exploitation of the technique for any kind of irradiation facility.

Results obtained with the single irradiation batch model, interpolating one step or two consecutive steps, are almost identical, therefore only the latter are analysed – in table 8 and Fig. 29 – even if the first are reported in table 7 and Fig. 28. Burn-up calculation outcomes are described in table 9 and Fig. 30.

The deviation between ALEPH and combined ALEPH and TDM isotopic composition, averaged over nuclides and materials is definitely low for the single irradiation batch (0.27%) – the same divergence found in the single-pin experiment REBUS using TDM for 13 steps – and a bit higher for two irradiation cycles (1.13%). More into detail, material concentrations are closer to ALEPH results the farer are located from the centre of the core – remembering that the used typical BOC configuration implies that the fresh fuel assemblies are loaded into the centre of the core, whereas most burned assemblies are in the periphery.

Respectively, the three materials, out of five, that are positioned in the outer layers, show nuclide averaged discrepancies of 0.008%, 0.015% and 0.023% for the single cycle model and 0.019%, 0.229% and 0.481% for two cycles, in descending order towards the edges.

Fresh fuel – that is placed in the centre of the core, where the neutron flux reaches its peak – and its surrounding material – that is burned fuel – have deviations that increase up to averaged values of 0.046% and 3.578%, respectively for the one and two irradiation batches configuration.

The discrepancies seem strictly related to the position and to the fuel burn-up – indeed, reaction rates change faster in the middle of the core, where materials are fresh, the flux higher and the burn-up still low and, at the same time, TDM and ALEPH outcomes present bigger divergences.

Nuclide cross sections, averaged onto a high-flux, do not undergo big variations, since their spectra sketch the major changes and resonances at thermal and epithermal energies. Therefore, it appears highly probable that, even though the TDM

implementation does not match the ALEPH inventory, it gives more accurate outcomes, since it succeeds in following time variations better than the case of constant coefficients. As a matter of fact, reaction rates do not experience scattered changes and their evolution may be described by a linear function. Unfortunately, the validation of these conclusions cannot be confirmed since experimental data are missing.

Results obtained making use of time-dependent matrixes for two steps underestimate, in general, concentrations obtained with a pure ALEPH calculation; only material located at the edge of the core matches with high-precision ALEPH results giving nuclide compositions slightly in excess.

3.2.1 Actinides

Actinides results generally coincide with ALEPH retrieved concentrations for every region of the core, that is, for every material. The observed deviations are of the same order of the averages, however they result even closer considering only uranium and plutonium nuclides, where they get really close to zero. The divergence derives especially from the Np-237, and to some percents from the isotopes of curium and Am-242*m*. Moreover, also the U-236 shows deviations slightly over the average for almost all materials. Since curium isotopes get far from ALEPH inventory underestimating it, it seems highly probable that the lack in accuracy present in the REBUS experiment for these nuclides is occurring again.

3.2.2 Fission products

Fission products deviations take over the nuclides averaged discrepancy between TDM and ALEPH outcomes for all materials, but the fresh fuel, where they are offset by the actinides.

As for all other isotopes they generally present lower values than the ALEPH inventory. Hence, the issue on the samarium isotope (Sm-148 in particular) prediction detected in the REBUS model, where both the burn-up calculations gave unexplainable lower concentrations, here are extended with a further negative contribution. However, again

because of the lack of experimental results, this is just an analysis based on the assumption that the wrong prediction of the samarium occurs.

3.2.3 Burn-up indicators

Burn-up indicators analysis results to be complicated because divergences are often offset and peaks appear without an actual physical occurrence. They follow the same behaviour described above, that is, bigger discrepancies come about for fresh material. However, deviations are really small: in the single cycle model they are even smaller of one order of magnitude than deviations obtained in the REBUS experiment. Therefore it can be stated that the TDM technique used for this model is greatly reliable for burn-up value computations.

Outcomes resulting from TDM technique are very close to the retrieved concentrations obtained by using the ALEPH code for the full irradiation cycle. Therefore, on the base of considerations just explained about coefficients evolution in presence of a high-flux, it can be assumed that reaction rate variations in time, in an irradiation field, are small and regular. This reasoning suggests a good performance of the pure ALEPH code, even if the matrix coefficients are constants, and an even more realistic depletion making use of the TDM method.

Table 7: Relative difference in percent between the calculated ALEPH2 and combined TDM and ALEPH2 isotopic inventory. The normalisation was done with regard to the concentration of U-238. The ALEPH2 and the combined TDM and ALEPH2 code were used with the MYRRHA critical core model for five materials (m204, m203, m202, m201 and m101) located in five different regions of the core, from the centre to the edge. The burn-up calculation was carried out for one irradiation cycle. Time-dependent coefficients were used for one step.

Nuclide	TDM (one interp. step - one irr. cycle) [%]				
	m204	m203	m202	m201	m101
U-234	0.00%	0.00%	0.00%	0.00%	0.00%
U-235	0.00%	0.00%	0.00%	0.00%	0.00%
U-236	-0.01%	0.01%	0.00%	0.01%	-0.01%
U-238	0.00%	0.00%	0.00%	0.00%	0.00%
Np-237	-0.13%	0.07%	0.04%	-0.01%	0.01%
Pu-238	0.00%	0.00%	0.00%	0.00%	0.00%
Pu-239	0.00%	0.00%	0.00%	0.00%	0.00%
Pu-240	0.00%	0.00%	0.00%	0.00%	0.00%
Pu-241	0.00%	0.00%	0.00%	0.00%	0.00%
Pu-242	0.00%	0.00%	0.00%	0.00%	0.00%
Am-241	0.00%	0.00%	0.00%	0.00%	0.00%
Am-242m	-0.01%	0.01%	-0.01%	0.01%	0.00%
Am-243	0.00%	-0.01%	-0.01%	0.00%	0.01%
Cm-242	-0.01%	0.01%	-0.02%	0.02%	-0.01%
Cm-243	-0.05%	-0.01%	0.00%	0.01%	-0.02%
Cm-244	0.02%	0.01%	-0.01%	0.00%	0.00%
Cm-245	0.05%	0.03%	0.01%	-0.01%	0.01%
Ce-144	0.02%	0.01%	-0.01%	0.00%	-0.01%
Nd-142	-0.22%	0.05%	0.00%	0.01%	-0.02%
Nd-143	0.01%	0.00%	0.00%	0.00%	0.00%
Nd-144	0.00%	0.00%	0.00%	0.00%	0.00%
Nd-145	0.02%	0.01%	-0.01%	0.00%	0.00%
Nd-146	0.01%	0.01%	-0.01%	0.00%	-0.01%
Nd-148	0.01%	0.01%	-0.01%	0.00%	-0.01%
Nd-150	0.01%	0.01%	-0.01%	0.00%	-0.01%
Sm-147	0.00%	0.00%	0.00%	0.00%	0.00%
Sm-148	-0.49%	0.09%	-0.04%	0.03%	0.02%
Sm-149	0.01%	0.01%	0.00%	0.00%	-0.01%
Sm-150	-0.04%	0.01%	-0.03%	0.02%	0.01%
Sm-151	0.01%	0.01%	-0.01%	0.00%	-0.01%
Sm-152	0.01%	0.01%	-0.01%	0.00%	0.00%
Sm-154	0.01%	0.01%	-0.01%	0.00%	-0.01%
Eu-153	0.02%	0.01%	-0.01%	-0.01%	-0.01%
Eu-154	-0.01%	0.02%	-0.01%	0.00%	0.01%
Eu-155	0.01%	0.01%	-0.01%	0.00%	0.00%
Gd-155	0.00%	0.00%	0.00%	0.00%	0.00%
Cs-133	0.01%	0.00%	0.00%	0.00%	0.00%
Cs-135	0.01%	0.01%	-0.01%	0.00%	-0.01%
Cs-137	0.01%	0.01%	-0.01%	0.00%	-0.01%
Mo-95	0.00%	0.00%	0.00%	0.00%	0.00%
Tc-99	0.01%	0.01%	-0.01%	0.00%	-0.01%
Ru-101	0.01%	0.01%	-0.01%	0.00%	-0.01%
Rh-103	0.00%	0.00%	0.00%	0.00%	0.00%
Pd-105	0.01%	0.01%	-0.01%	0.00%	-0.01%
Pd-108	0.01%	0.00%	-0.01%	0.00%	-0.01%
Ag-109	0.01%	0.00%	-0.01%	0.00%	-0.01%

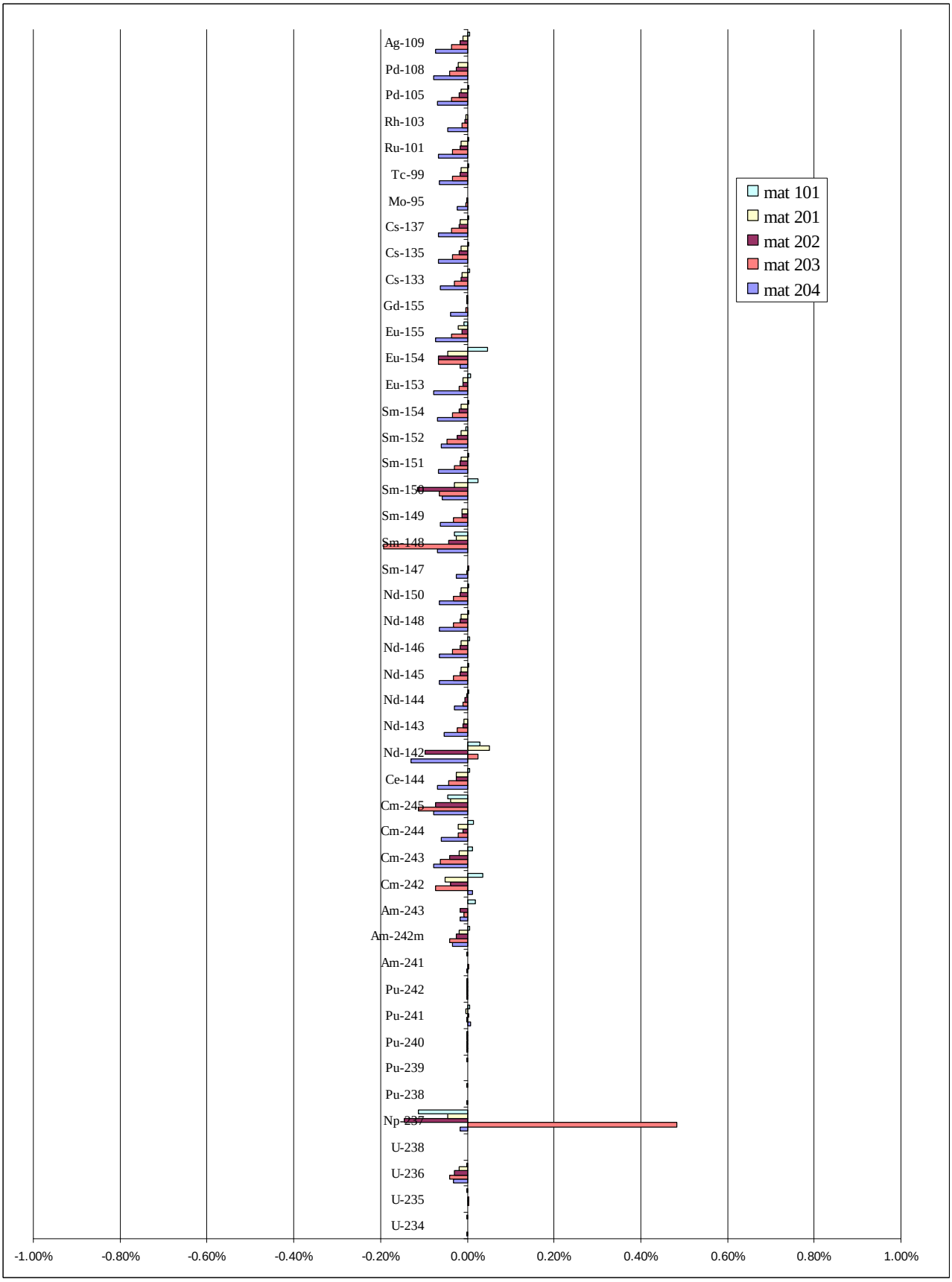

Figure 28: Comparison of ALEPH2 and coupled TDM and ALEPH2 code for the MYRRHA critical core model. The burn-up calculation was carried out for one irradiation cycle. Time-dependent coefficients were used for one steps. See also table 7.

Table 8: Relative difference in percent between the calculated ALEPH2 and combined TDM and ALEPH2 isotopic inventory. The normalisation was done with regard to the concentration of U-238. The ALEPH2 and the combined TDM and ALEPH2 code were used with the MYRRHA critical core model for five materials (m204, m203, m202, m201 and m101) located in five different regions of the core, from the centre to the edge. The burn-up calculation was carried out for one irradiation cycle. Time-dependent coefficients were used for two steps.

Nuclide	TDM (two interp. steps - one irr. cycle) [%]				
	m204	m203	m202	m201	m101
U-234	0.00%	0.00%	0.00%	0.00%	0.00%
U-235	0.00%	0.00%	0.00%	0.00%	0.00%
U-236	-0.03%	-0.04%	-0.03%	-0.02%	0.00%
U-238	0.00%	0.00%	0.00%	0.00%	0.00%
Np-237	-0.02%	0.48%	-0.15%	-0.05%	-0.11%
Pu-238	0.00%	0.00%	0.00%	0.00%	0.00%
Pu-239	0.00%	0.00%	0.00%	0.00%	0.00%
Pu-240	0.00%	0.00%	0.00%	0.00%	0.00%
Pu-241	0.01%	0.00%	0.00%	0.00%	0.01%
Pu-242	0.00%	0.00%	0.00%	0.00%	0.00%
Am-241	0.00%	0.00%	0.00%	0.00%	0.00%
Am-242m	-0.03%	-0.04%	-0.03%	-0.02%	0.01%
Am-243	-0.02%	-0.01%	-0.02%	0.00%	0.02%
Cm-242	0.01%	-0.07%	-0.04%	-0.05%	0.04%
Cm-243	-0.08%	-0.06%	-0.04%	-0.02%	0.01%
Cm-244	-0.06%	-0.02%	-0.01%	-0.02%	0.01%
Cm-245	-0.08%	-0.11%	-0.07%	-0.04%	-0.04%
Ce-144	-0.07%	-0.04%	-0.03%	-0.02%	0.01%
Nd-142	-0.13%	0.03%	-0.10%	0.05%	0.03%
Nd-143	-0.05%	-0.02%	-0.01%	-0.01%	0.00%
Nd-144	-0.03%	-0.01%	-0.01%	0.00%	0.00%
Nd-145	-0.06%	-0.03%	-0.02%	-0.01%	0.00%
Nd-146	-0.06%	-0.03%	-0.02%	-0.01%	0.00%
Nd-148	-0.06%	-0.03%	-0.02%	-0.01%	0.00%
Nd-150	-0.06%	-0.03%	-0.02%	-0.01%	0.00%
Sm-147	-0.02%	0.00%	0.00%	0.00%	0.00%
Sm-148	-0.07%	-0.19%	-0.04%	-0.03%	-0.03%
Sm-149	-0.06%	-0.03%	-0.01%	-0.01%	0.00%
Sm-150	-0.06%	-0.06%	-0.11%	-0.03%	0.03%
Sm-151	-0.07%	-0.03%	-0.02%	-0.01%	0.00%
Sm-152	-0.06%	-0.05%	-0.02%	-0.01%	0.00%
Sm-154	-0.07%	-0.03%	-0.02%	-0.01%	0.00%
Eu-153	-0.08%	-0.02%	-0.01%	-0.01%	0.01%
Eu-154	-0.02%	-0.07%	-0.07%	-0.04%	0.05%
Eu-155	-0.07%	-0.04%	-0.01%	-0.02%	-0.01%
Gd-155	-0.04%	0.00%	0.00%	0.00%	0.00%
Cs-133	-0.06%	-0.03%	-0.01%	-0.01%	0.00%
Cs-135	-0.07%	-0.03%	-0.02%	-0.01%	0.00%
Cs-137	-0.07%	-0.04%	-0.02%	-0.02%	0.00%
Mo-95	-0.02%	0.00%	0.00%	0.00%	0.00%
Tc-99	-0.06%	-0.03%	-0.02%	-0.01%	0.00%
Ru-101	-0.07%	-0.03%	-0.02%	-0.01%	0.00%
Rh-103	-0.05%	-0.01%	-0.01%	0.00%	0.00%
Pd-105	-0.07%	-0.04%	-0.02%	-0.02%	0.00%
Pd-108	-0.08%	-0.04%	-0.02%	-0.02%	0.00%
Ag-109	-0.07%	-0.04%	-0.02%	-0.01%	0.01%

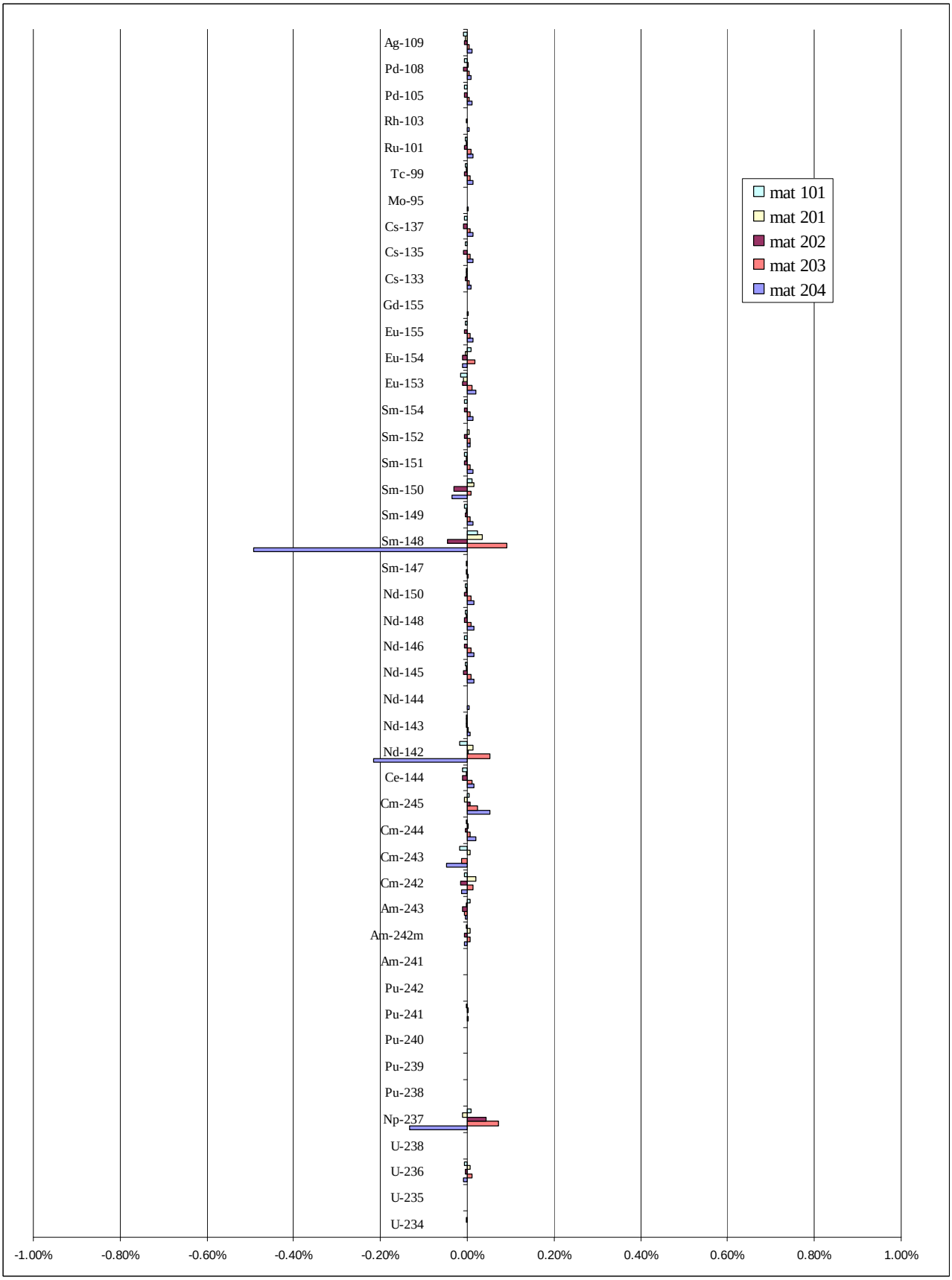

Figure 29: Comparison of ALEPH2 and coupled TDM and ALEPH2 code for the MYRRHA critical core model. The burn-up calculation was carried out for one irradiation cycle. Time-dependent coefficients were used for two steps. See also table 7.

Table 9: Relative difference in percent between the calculated ALEPH2 and combined TDM and ALEPH2 isotopic inventory. The normalisation was done with regard to the concentration of U-238. The ALEPH2 and the combined TDM and ALEPH2 code were used with the MYRRHA critical core model for five materials (m204, m203, m202, m201 and m101) located in five different regions of the core, from the centre to the edge. The burn-up calculation was carried out for two irradiation cycle. Time-dependent coefficients were used for four steps.

Nuclide	TDM (four interp. steps – two irr. cycle) [%]				
	m204	m203	m202	m201	m101
U-234	0.27%	0.18%	0.10%	0.06%	0.02%
U-235	0.38%	0.26%	0.14%	0.07%	0.02%
U-236	-2.99%	-1.19%	-0.35%	-0.07%	0.00%
U-238	0.21%	0.15%	0.09%	0.06%	0.01%
Np-237	-3.72%	-0.97%	-0.59%	-0.39%	-0.04%
Pu-238	0.33%	0.23%	0.13%	0.08%	0.01%
Pu-239	0.29%	0.20%	0.11%	0.07%	0.01%
Pu-240	0.17%	0.13%	0.09%	0.07%	0.01%
Pu-241	0.21%	0.15%	0.11%	0.07%	0.02%
Pu-242	0.24%	0.17%	0.10%	0.07%	0.01%
Am-241	0.39%	0.27%	0.14%	0.08%	0.01%
Am-242m	-2.79%	-1.18%	-0.40%	-0.12%	0.01%
Am-243	-0.77%	-0.37%	-0.11%	0.02%	0.02%
Cm-242	-5.25%	-2.78%	-1.19%	-0.48%	0.00%
Cm-243	-6.79%	-2.20%	-0.44%	-0.04%	-0.02%
Cm-244	-4.28%	-1.25%	-0.32%	-0.06%	0.02%
Cm-245	-7.72%	-2.47%	-0.79%	-0.17%	-0.07%
Ce-144	-5.61%	-2.67%	-1.23%	-0.65%	0.01%
Nd-142	-6.59%	-2.65%	-0.46%	0.14%	0.02%
Nd-143	-4.51%	-1.77%	-0.69%	-0.32%	0.01%
Nd-144	-2.27%	-0.61%	-0.17%	-0.05%	0.01%
Nd-145	-4.68%	-1.85%	-0.72%	-0.33%	0.01%
Nd-146	-4.73%	-1.86%	-0.71%	-0.31%	0.01%
Nd-148	-4.72%	-1.86%	-0.72%	-0.33%	0.01%
Nd-150	-4.69%	-1.83%	-0.71%	-0.31%	0.01%
Sm-147	-1.60%	-0.35%	-0.11%	-0.05%	0.02%
Sm-148	-4.61%	-0.97%	0.30%	0.56%	-0.11%
Sm-149	-4.65%	-1.85%	-0.75%	-0.37%	0.02%
Sm-150	-5.16%	-1.36%	0.11%	0.51%	-0.01%
Sm-151	-4.62%	-1.83%	-0.76%	-0.38%	0.01%
Sm-152	-4.75%	-1.91%	-0.71%	-0.30%	-0.01%
Sm-154	-4.62%	-1.80%	-0.68%	-0.30%	0.01%
Eu-153	-4.56%	-1.67%	-0.61%	-0.23%	0.06%
Eu-154	-6.36%	-2.02%	-0.32%	0.20%	0.04%
Eu-155	-4.79%	-1.95%	-0.78%	-0.38%	-0.01%
Gd-155	-1.86%	-0.38%	-0.09%	-0.04%	0.01%
Cs-133	-4.67%	-1.86%	-0.72%	-0.33%	0.01%
Cs-135	-4.70%	-1.87%	-0.73%	-0.33%	0.01%
Cs-137	-4.71%	-1.88%	-0.73%	-0.33%	0.01%
Mo-95	-1.74%	-0.49%	-0.16%	-0.06%	0.01%
Tc-99	-4.66%	-1.85%	-0.72%	-0.33%	0.01%
Ru-101	-4.67%	-1.85%	-0.72%	-0.32%	0.02%
Rh-103	-3.42%	-1.19%	-0.42%	-0.17%	0.01%
Pd-105	-4.61%	-1.81%	-0.70%	-0.31%	0.01%
Pd-108	-4.69%	-1.85%	-0.71%	-0.32%	0.01%
Ag-109	-4.55%	-1.78%	-0.67%	-0.28%	0.02%

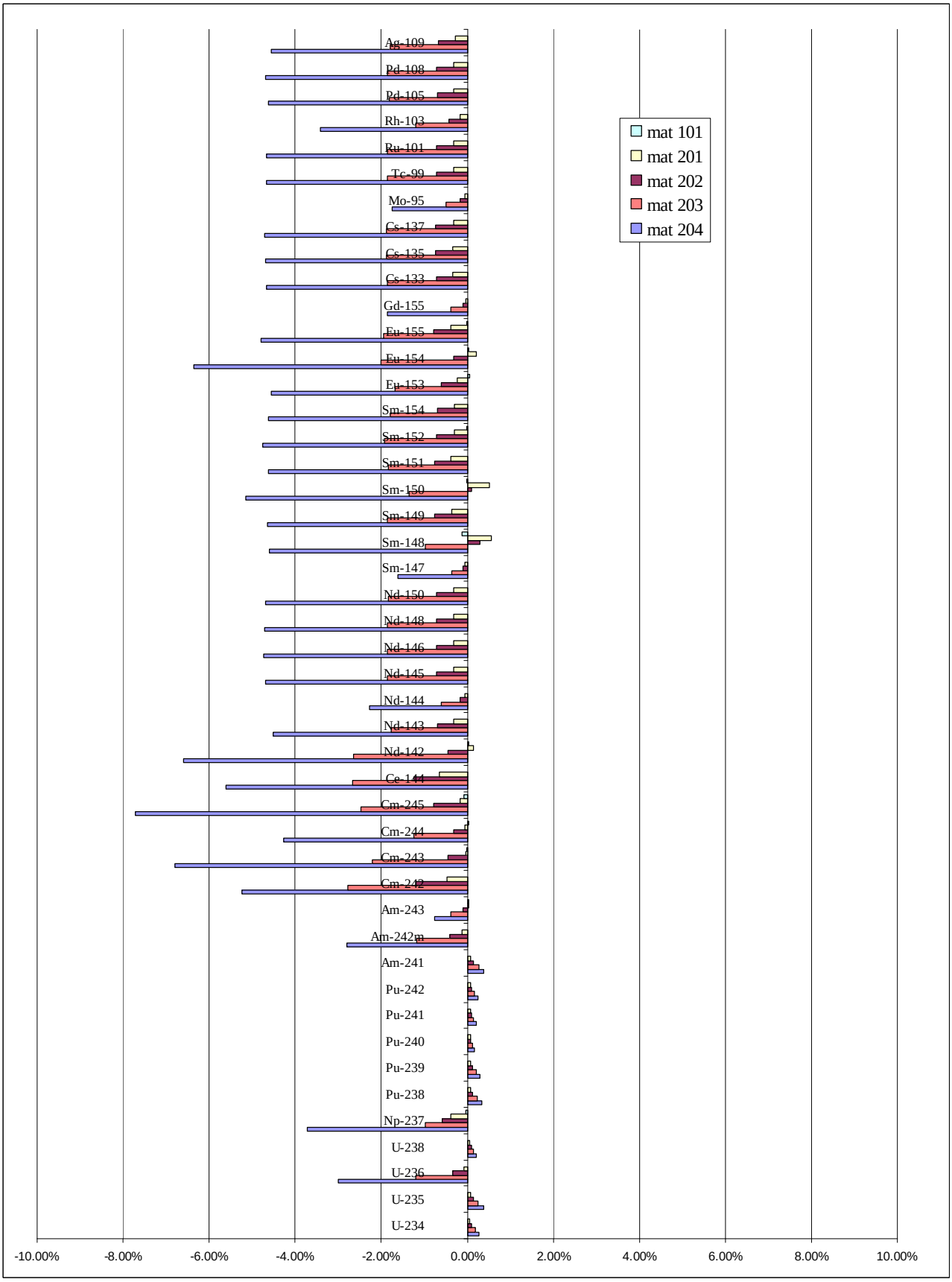

Figure 30: Comparison of ALEPH2 and coupled TDM and ALEPH2 code for the MYRRHA critical core model. The burn-up calculation was carried out for two irradiation cycle. Time-dependent coefficients were used for four steps. See also table 7.

Chapter 4

Conclusions and recommendations

The outstanding feature that has been developed is deemed completely satisfactory in solving Monte-Carlo burn-up calculations, both considering CPU running-time and accuracy of the isotopic inventory. The obtained results are so remarkable in their comparison with the full genuine version 2 of ALEPH, that it seems highly profitable to apply the time-dependent matrix method in combination with the current ALEPH2 to develop a further improvement of the code.

One of its main achievements is obtained in the accuracy of depletion calculation results, that is, the nuclide inventory retrieved after the irradiation history. The TDM method, by using reaction-rates that change in time throughout irradiation, owns an intrinsic feature that allows it to better follow the kinetic evolution of material in time, resulting in profoundly accurate outcomes.

The second and main accomplishment is the computational time reduction. One more time, it is relevant to point out the enormous difference in required CPU time between the steady-state and the dynamic part of the code. Indeed, for a typical burn-up problem, the most of the time is consumed by the neutronic calculation, while only few percents are used to deplete the fuel. The TDM severely reduces the computational time avoiding continuous MCNP(X) launches, however, the gain in time is strictly proportional to the number of steps in which time-dependent effective reaction rates are applied.

In this thesis work, a deep analysis of matrix coefficient variations throughout irradiation periods, carried out on a typical MOX fuel pin of a 17x17 PWR core, depicted a regular

development of reaction rates that can be easily predicted by using low-order polynomials and, in particular, linear functions as implemented in the TDM technique.

Two different approaches has been attempted to validate the method: the REBUS experimental benchmark and the MYRRHA critical core configuration. Concerning the first, both a single pin configuration and a full fuel assembly have been reproduced. Their results agree very well with the experimental data in both the two models, exceeding the precision obtained with the pure ALEPH 2 burn-up calculation and, at the same time, cutting almost 30% off the computational time. On the other hand, the surprising discrepancies encountered with ALEPH2 for some important radionuclides are still not overcome, even if several of them are slightly reduced.

The time-dependent matrix application to the MYRRHA critical core model gives very good outcomes, too. Making a restricted use of the TDM technique, in combination with ALEPH2, comes out in deviations from the pure ALEPH2 results that are almost insignificant. For longer periods, like the case of two batches, discrepancies increase, but it is arduous to understand whether the TDM nuclide concentration get closer or farer to the real situation, because of the lack in experimental data. However, the relatively small variations that reaction rates undergo in this context imply that the TDM technique is highly reliable also for high neutron flux models.

Although no limitation has been imposed on the number of steps wherein time-dependent matrixes are suitable to be applied, since the only restriction was a reasonable match of the trend of parameters with a first-degree polynomial function, the user is advised to make use of the TDM technique for a restricted amount of consecutive time intervals that amounts to a top-limit of four. Moreover, the operation of the method relies on a high precision of the coupled code (ALEPH) for the previous steps, in order to meet a linear behaviour of the matrix coefficients.

The finest results, obtained by the testing of the TDM technique, suggest its implementation in the ALEPH code, first by extrapolating the coefficients of the linear functions on the base of matrix coefficient behaviours that suitably fit, then by interpolating the effective reaction rates for the following step or further consecutive steps.

Bibliography

[1] Haeck, W., Verboomen, B., "*ALEPH 1.1.2 – a Monte carlo Burn-up Code*". BLG-1003, SCK•CEN, Belgium (2006).

[2] Booth, T. E., et al., (X-5 Monte Carlo Team), "*MCNP — A General Monte Carlo N-Particle Transport Code, Version 5, Volume II: User's Guide*". LA-CP-03-0245, Los Alamos National Laboratory (2003).

[3] Croff, A.G., "A *User's Manual for the ORIGEN2 Computer Code*". ORNL/TM-7175, Oak Ridge National Laboratory (1980).

[4] Xu, Z., Hejzlar, P., Driscoll, M.J., Kazimi, M.S., "*An improved MCNP-ORIGEN depletion program (MCODE) and its verification for high burn-up applications*". Proc. of the Int. Conf. PHYSOR, Seoul (2002).

[5] Poston, D.L. and Trellue, H.R., "*User's Manual, Version 2.0 for MONTEBURNS Version 1.0*". LA-UR-99-4999, Los Alamos National Laboratory (1999).

[6] Tippayakul, C., Ivanov, K., Misu, S., "*Improvements of MCOR: a Monte Carlo Depletion Code System for Fuel Assembly Reference Calculations*". PHYSOR-2006, Vancouver (2006).

[7] Pelowitz, D. B., ed., "*MCNPX User's Manual, Version 2.6.0*". LA-CP-07-1473, Los Alamos National Laboratory (2008)

[8] Pelowitz D.B., et al., "*MCNPX 2.7.C Extensions*". LA-UR-10-00481, Los Alamos National Laboratory (2010).

[9] Hairer, E., Wanner, G., "*Solving Ordinary Differential Equations. Stiff and Differential-Algebraic Problems. 2nd ed.*". Springer Series in Comput. Math., Vol. 14 (1996).

[10] Stankovskiy, A. and Van den Eynde, G., "*ALEPH 2.1 – A Monte Carlo Burn-up Code*". SCK•CEN Restricted Contract Report, SCK•CEN-R-5267 (2011).

[11] Wilson, W. B., et al., "*CINDER'90 code for Transmutation Calculations*". Proc. Int. Conf. on Nuclear Data for Science and Technology, Trieste, 1454 (1997).

[12] Cetnar, J., et al., "*General solution of bateman equations for nuclear transmutations*". Ann. Nucl. En., 33, 640 (2006).

[13] Pusa, M., Leppänen, J., "*Computing the matrix exponential in burnup calculations*". Nucl. Sci. Eng., 164, 140-150 (2010).

[14] Leppänen, J., "*Serpent Progress Report 2009*". VTT-R-01296-10, VTT Technical Research Centre of Finland (2010).

[15] Stankovskiy, A., Van den Eynde, G. and Vidmar, T., "*Development and validation of ALEPH Monte Carlo burn-up code*". Nuclear measurements; evaluations and applications, OECD/NEA, 161-170, SCK•CEN, Mol (2011).

[16] Abderrahim, H. A., "*MYRRHA – Science Towards Sustainability*". AccApp09, International Topical Meeting, Vienna (2009).

[17] E. Koonen, F. Joppen, P. Gubel, "*Safety challenges encountered during the operating life of the almost 40 years old research reactor BR2*". IAEA-CN-82: International Conference on Topical Issues in Nuclear Safety, Vienna (2001).

[18] Bateman, H., "*Solution of a system of differential equations occurring in the theory of radio-active transformations*". Math. Proc. Cambridge 15, 423-427 (1910).

[19] Haeck, W. and Verboomen, B., "*An optimum approach to Monte Carlo Burnup*". Nucl. Sci. Eng., 156, 180-196 (2007).

[20] Higham, N. J., "*The Scaling and Squaring Method for the Matrix Exponential Revisited*". SIAM J. Matrix Anal. Appl., Vol. 26, 1179-1193 (2005).

[21] Moler, C., and Van Loan, C., "*Nineteen Dubious Ways to Compute the Exponential of a Matrix, Twenty-Five Years Later*". SIAM Rev., 45 (2003).

[22] Gauld, C., Hermann, O. W., and Westfall, R. M., "*ORIGEN-S: SCALE system module to calculate fuel depletion, actinide transmutation, fission product buildup and decay, and associated radiation source terms, SCALE6 Manual*". ORNL/TM-2005/39, Version 6, Vol. II, Sect. F7, Oak Ridge National Laboratory (2009).

[23] Yamamoto, A., Tatsumi, M. and Sugimura, N., "*Numerical Solution of Stiff Burnup Equations with Short Half Lived Nuclides by the Krylov Subspace Method*". J. Nucl. Sci. Technol., 44, 2, 147 (2007).

[24] Baker, G. A. Jr., "*Essentials of Padé Approximants in Theoretical Physics*". Academic Press, 27-38, New York (1975).

[25] Cetnar, J., "*General solution of Bateman equations for nuclear transmutations*". Ann. Nucl. Energy 33, 640-645 (2006).

[26] Isotalo, A. E. and Aarnio, P. A., "*Comparison of depletion algorithms for large systems of nuclides*". Ann. Nucl. Energy 38, 261-268 (2011).

[27] Cody, W. J., Meinardus, G. and Varga, R. S., "*Chebyshev Rational Approximations to e-x in [0,∞) and Applications to Heat-Conduction Problems*". J. Approx. Theory, 2, 50 (1969).

[28] Pusa, M., "*Rational Approximations to the Matrix Exponential in Burnup Calculations*". Nucl. Sci. Eng. 169, 155-167 (2011).

[29] Petzold, L.R., "*Automatic Selection of Methods for Solving Stiff and Nonstiff Systems of Ordinary Differential Equations*", Siam J. Sci. Stat. Comput., 4, 136-148 (1983).

[30] Stankovskiy, A. and Van den Eynde, G., "*Advanced Method for Calculations of Core Burn-up, Activation of Structural Materials and Spallation Products Accumulation in Accelerator Driven Systems*". Science and Technology of Nuclear Installations, vol. 2012, Article ID 545103, 12 pages (2012). doi:10.1155/2012/545103

[31] Hindmarsh, A. C., "*ODEPACK, A systematized Collection of ODE Solvers, in Scientific Computing*". Stepleman, R. S., et al. (Eds.), North-Holland, Amsterdam, 55-64 (1984).

[32] O'Connor, G. J. and Liem, P. H., "*Burn-up Credit Criticality Benchmark – Phase IV-B: Results and Analysis of MOX Fuel Depletion Calculations*". ISBN 92-64-02124-8, Nucl. Sci., NEA/NSC/DOC (2003).

[33] Isotalo, A. E. and Aarnio, P. A., "*Substep methods for burnup calculations with Bateman solutions*". Ann. Nucl. Energy 38, 2509-2514 (2011).

[34] Todosow, M. and Kazimi, M., "*Optimization of Heterogeneous Utilization of Thorium in PWRs to Enhance Proliferation Resistance and Reduce Waste*". BNL-73152-2004, Brookhaven National Laboratory (2004).

[35] Leppänen, J., "*PSG2/Serpent – A continuous-Energy Monte Carlo Reactor Physics Burnup Calculation Code, User's Manual*". VTT Technical Research Centre of Finland, < http://montecarlo.vtt.fi > (accessed 12.12.2010).

[36] Koning, A., et al., "The *JEFF-3.1 Nuclear Data Library*". JEFF Report 21, Nuclear Energy Agency Data Bank, OECD (2006).

[37] Lance, B., "*REBUS International Programme*". REBUS-PWR Final Report, Ref. No. File 0501320/221-1 (RE 2005/37), SCK•CEN, Belgium (2004).

[38] Vidmar, T., Stankovskiy, A. and Van den Eynde, G., "*ALEPH2 and the REBUS Data – Comparison of REBUS Experimental Results of Fuel Burn-up with ALEPH2 Calculations*". Internal Report SCK•CEN-I-203, Belgium (2010).

[39] Malambu, E. and Stankovskiy, A., "*Proposal for MYRRHA Core Configurations with 30 at%(Pu, Am)-enriched MOX Fuel*". Internal Report SCK•CEN-I-260, Belgium (2012).

List of figures

List of tables

Appendixes

Disappearance rate evolution throughout irradiation time for a single-pin model of a typical 17x17 PWR fuel assembly. The MCNP(X) calculation has been performed using 50000 neutron histories per cycle for 230 cycles.

A.1 U-235 disappearance rate evolution throughout irradiation time.

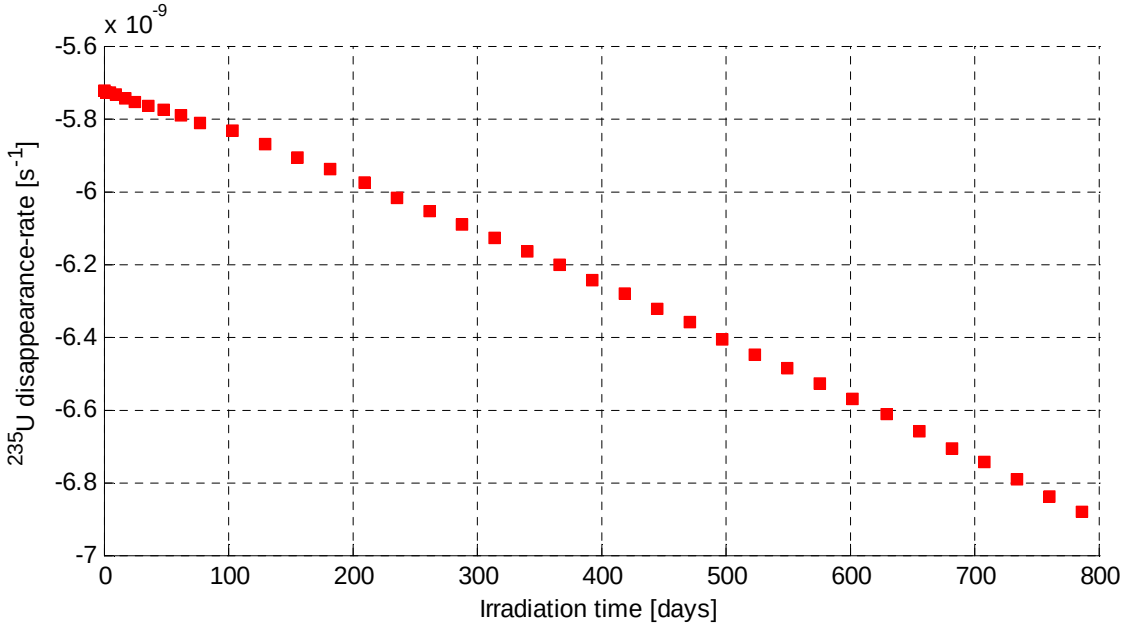

A.2 U-235 radiative capture rate evolution throughout irradiation time

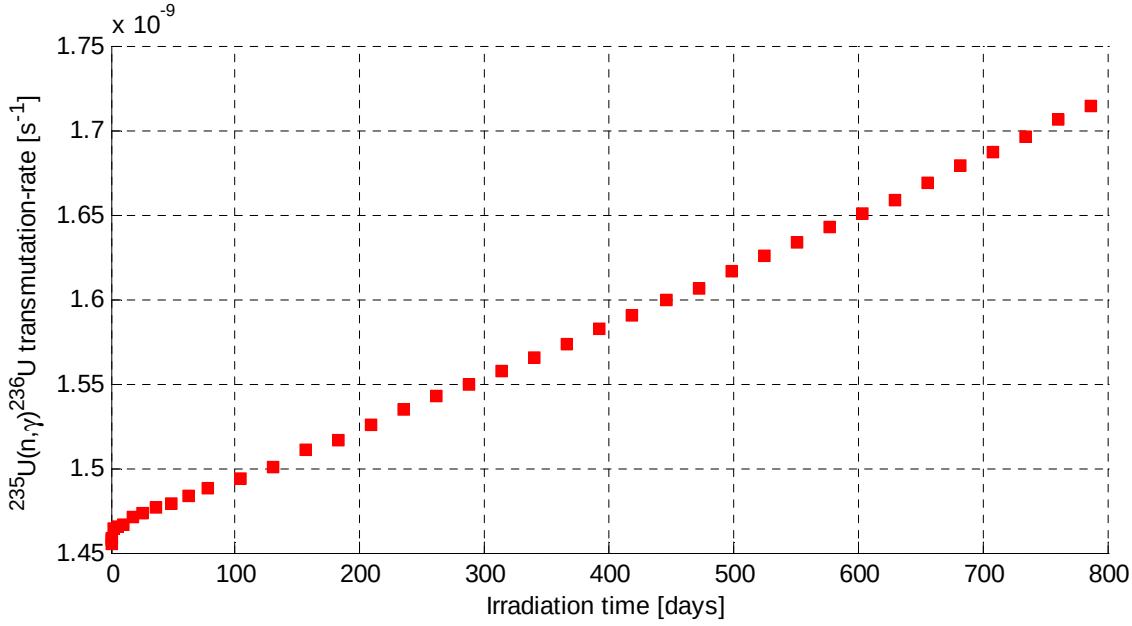

A.3 U-238 disappearance rate evolution throughout irradiation time

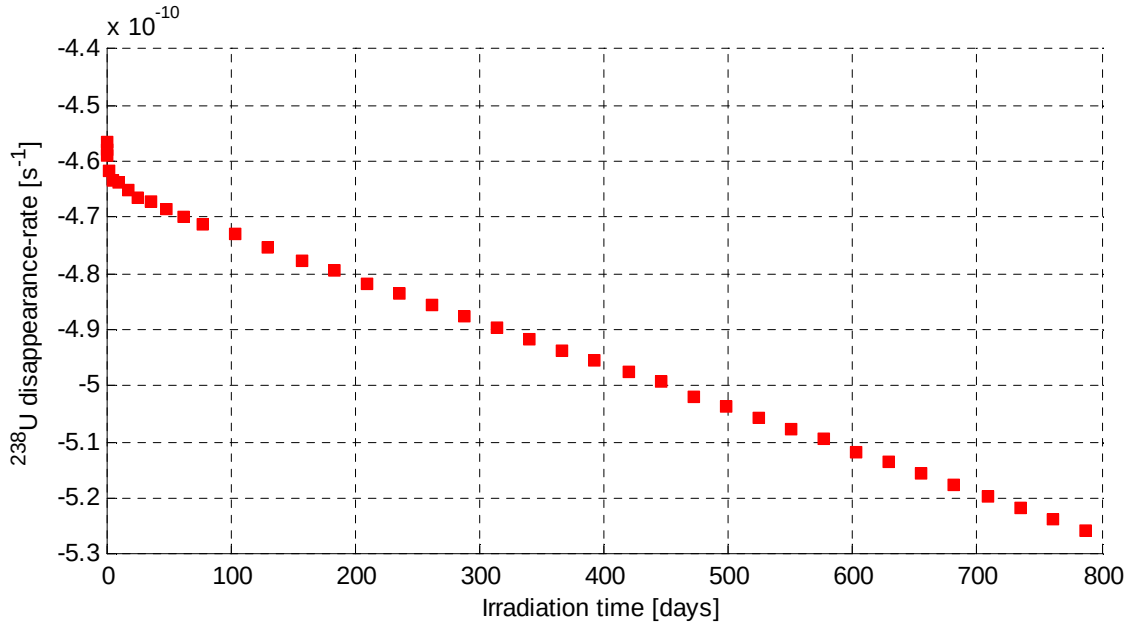

A.4 Pu-239 disappearance rate evolution throughout irradiation time

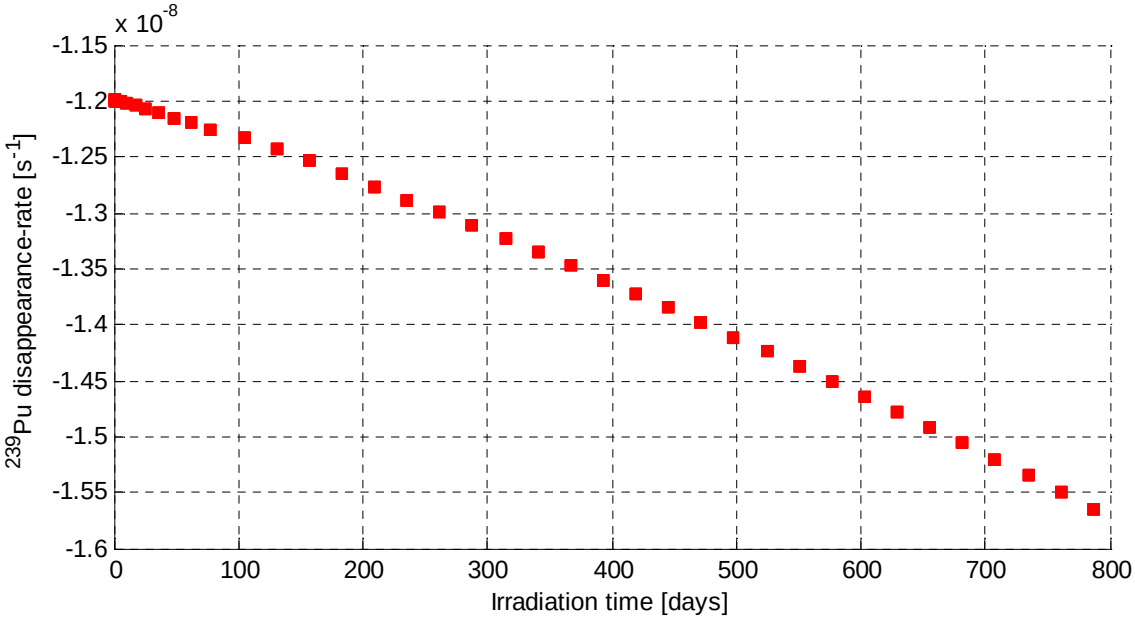

A.5 Pu-239 radiative capture rate evolution throughout irradiation time

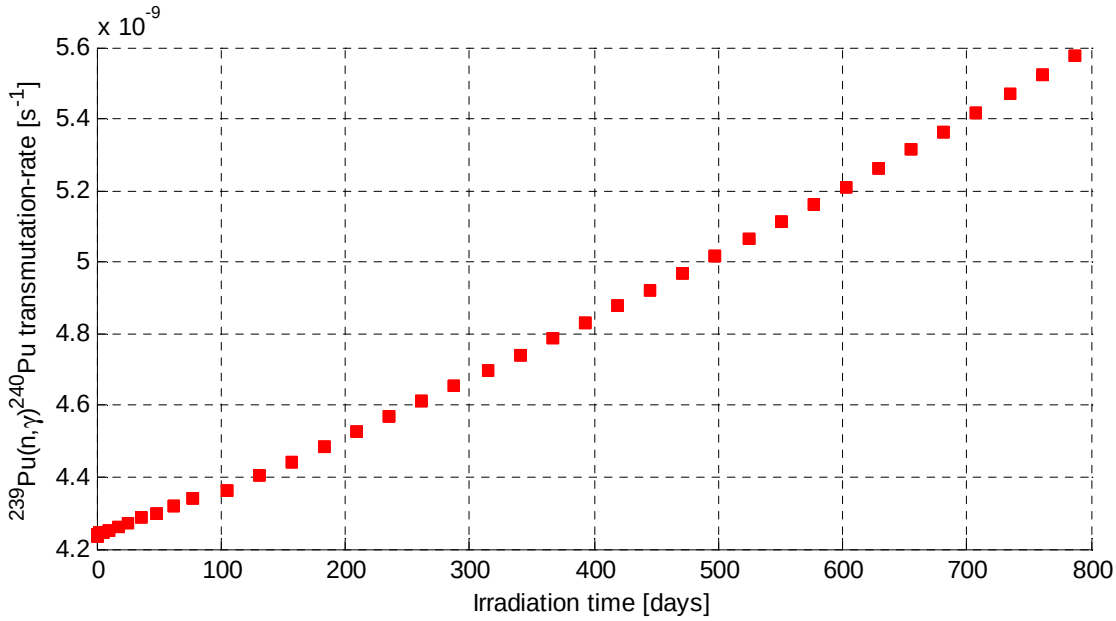

A.6 Pu-240 disappearance rate evolution throughout irradiation time

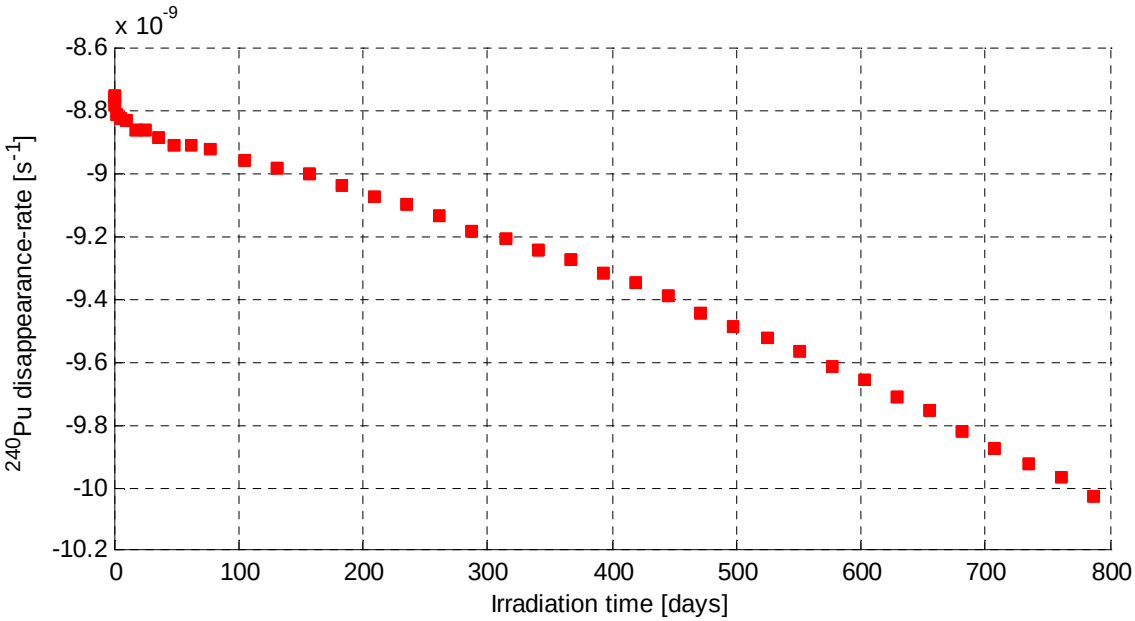

A.7 U-240 radiative capture rate evolution throughout irradiation time

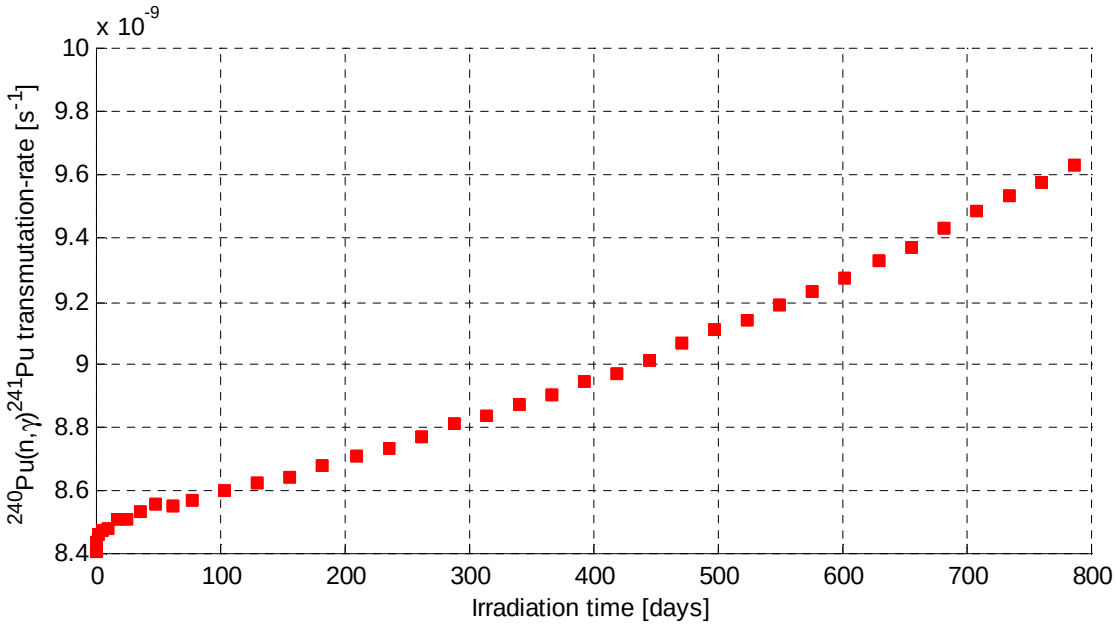

A.8 Pu-241 disappearance rate evolution throughout irradiation time

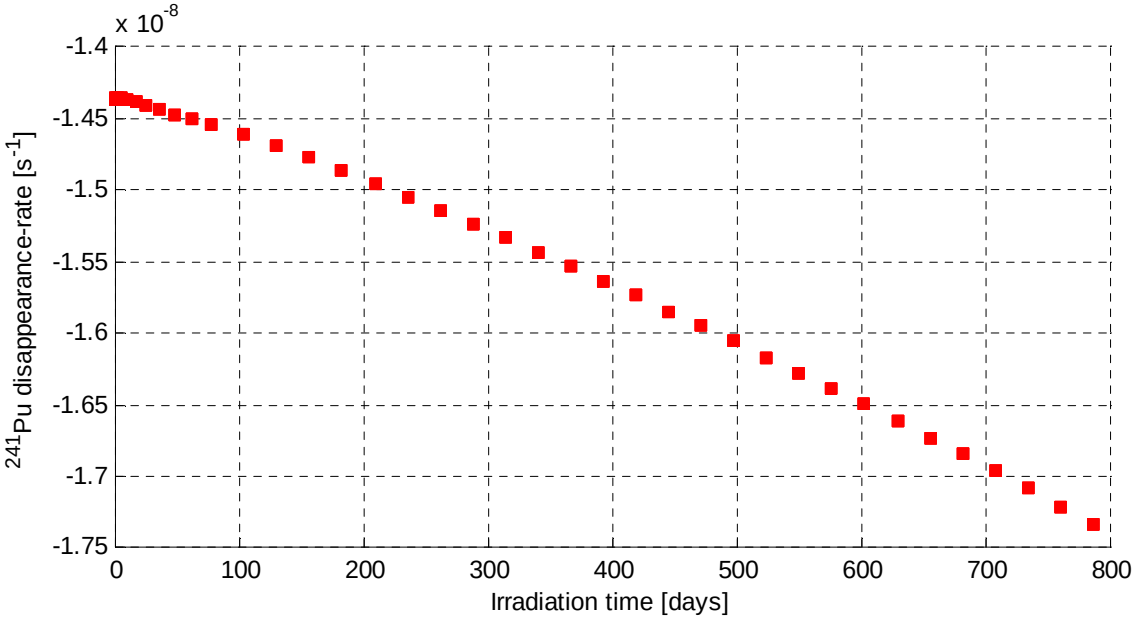

A.9 Pu-241 radiative capture rate evolution throughout irradiation time

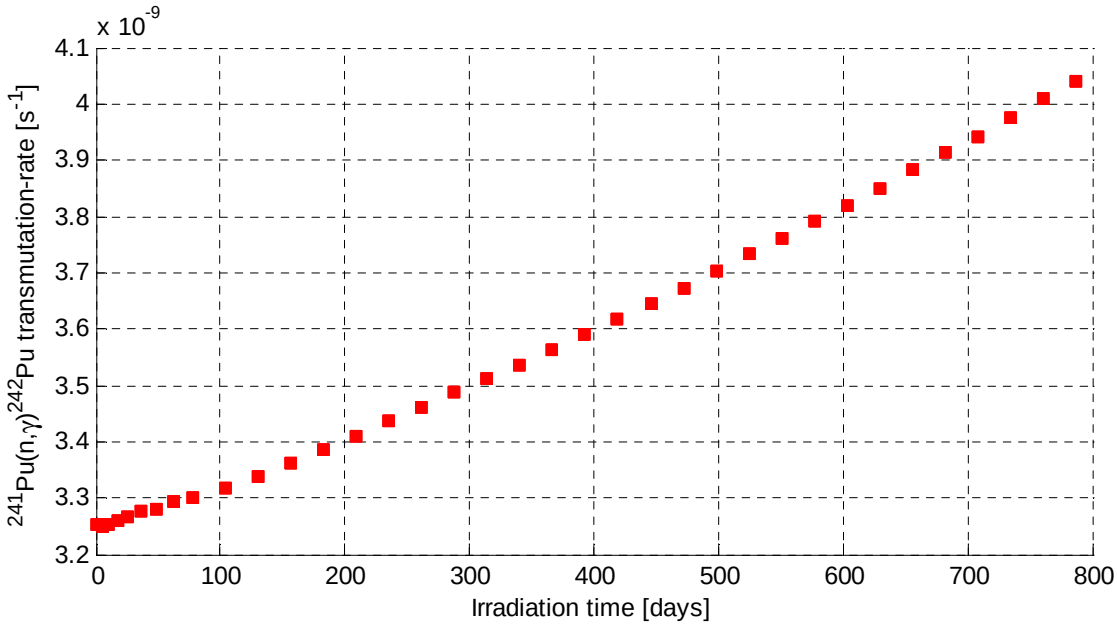

A.10 Pu-242 radiative capture rate evolution throughout irradiation time

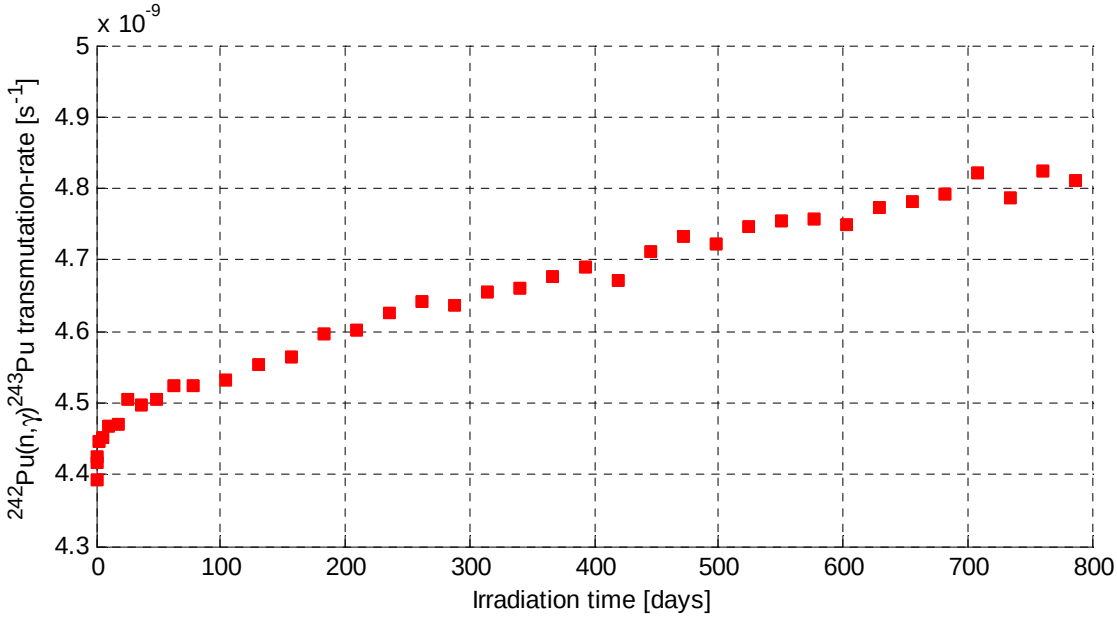

A.11 Xe-135 disappearance rate evolution throughout irradiation time

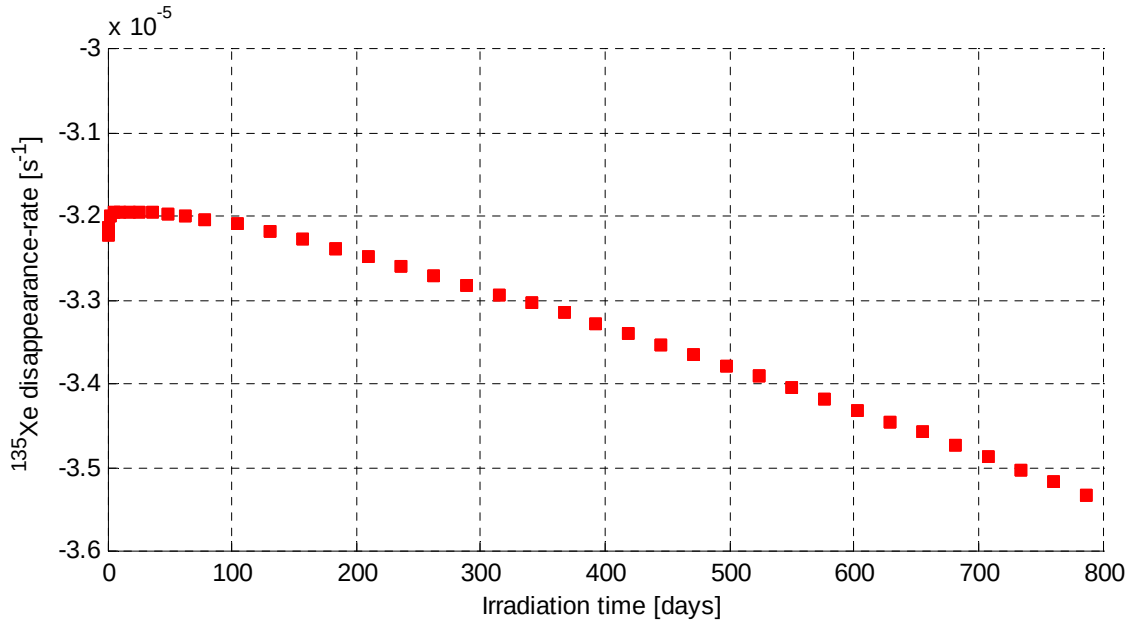

A.12 Xe-135 radiative capture rate evolution throughout irradiation time

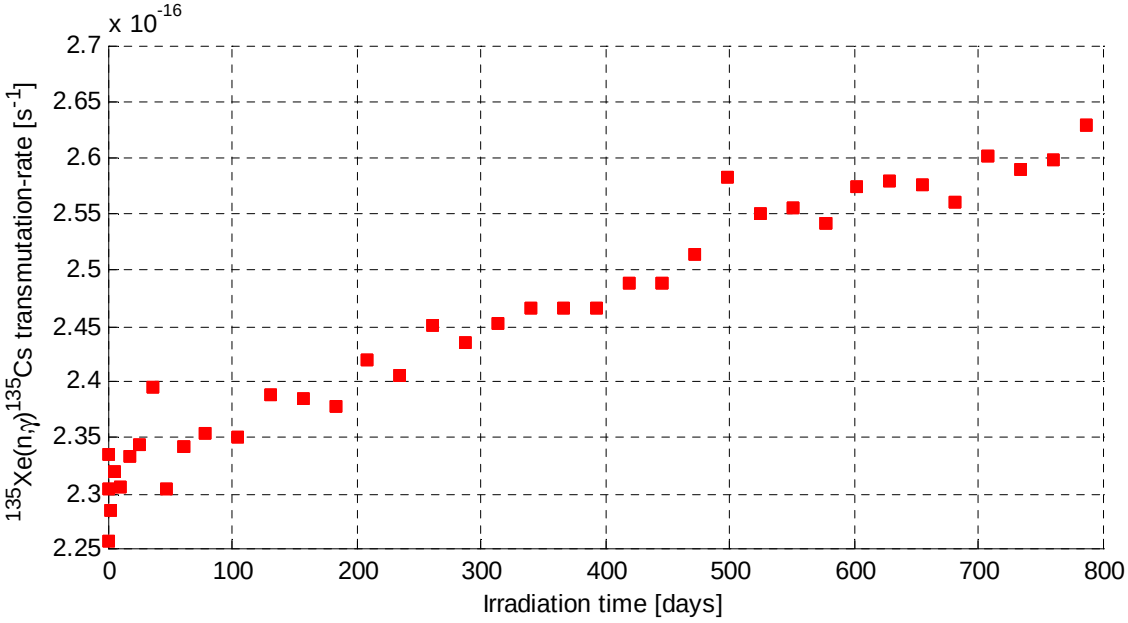

A.13 Nd-148 disappearance rate evolution throughout irradiation time

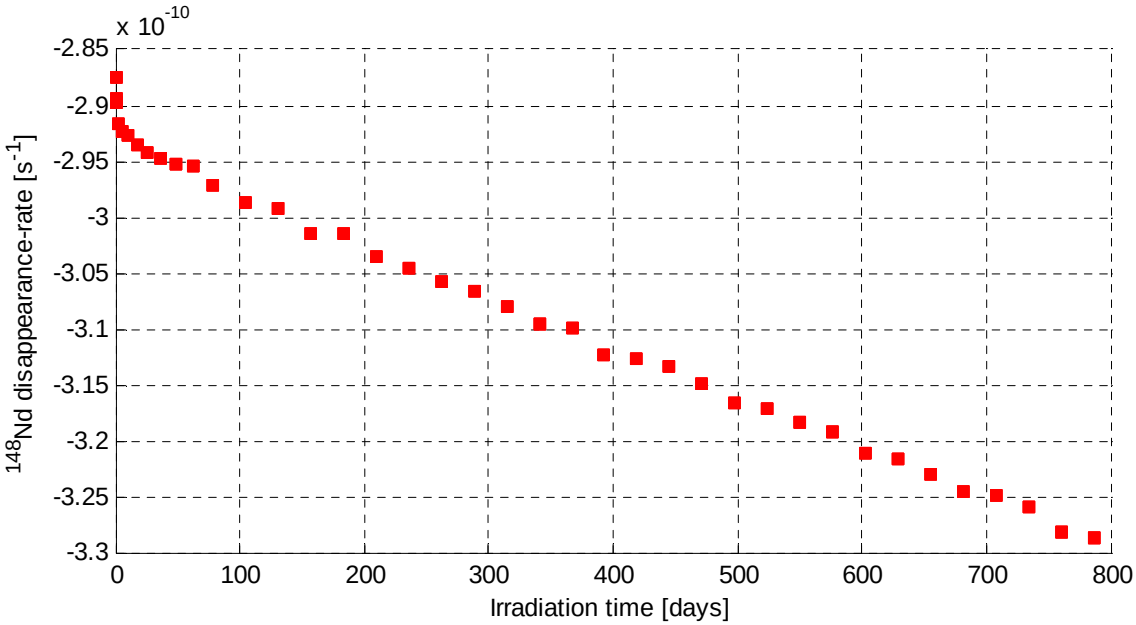

A.14 Sm-149 disappearance rate evolution throughout irradiation time

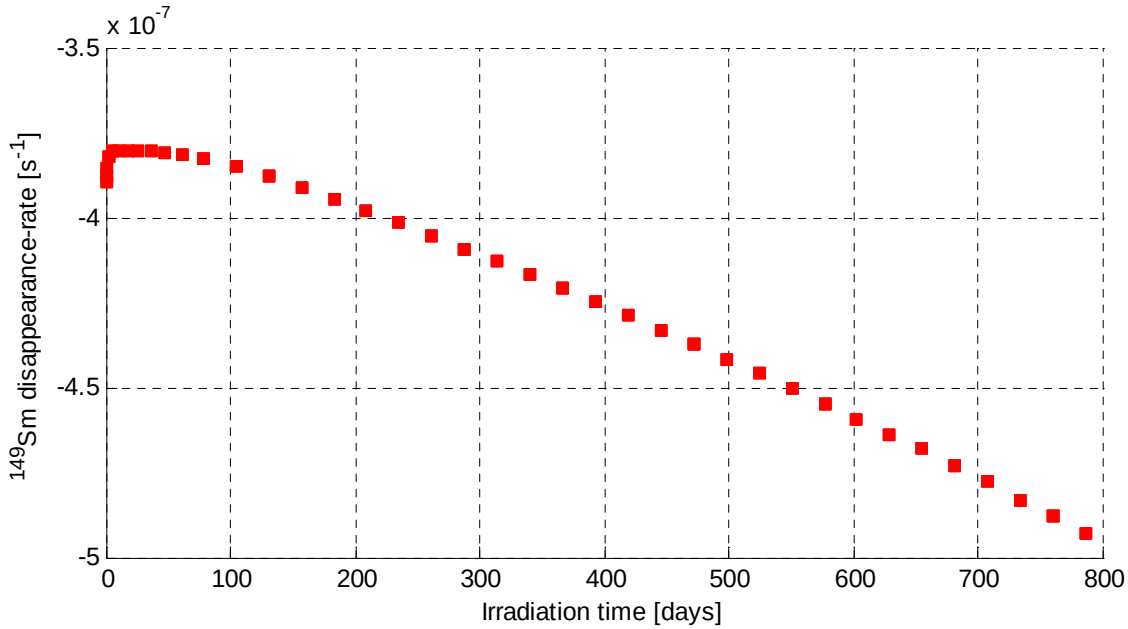

A.15 Gd-155 disappearance rate evolution throughout irradiation time

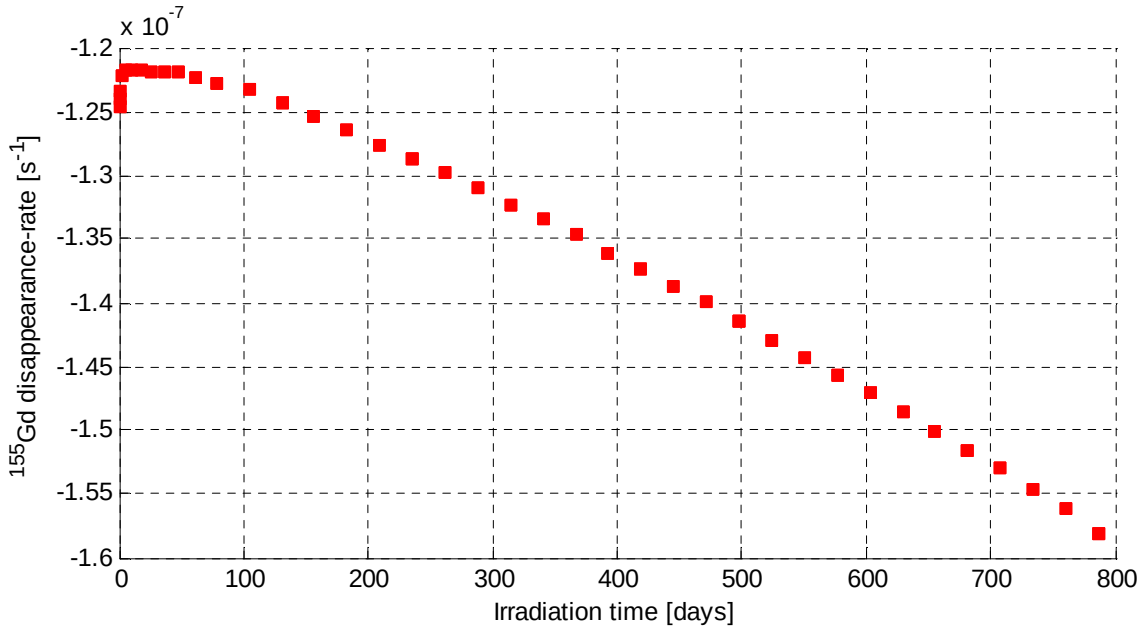

A.16 Am-241 disappearance rate evolution throughout irradiation time

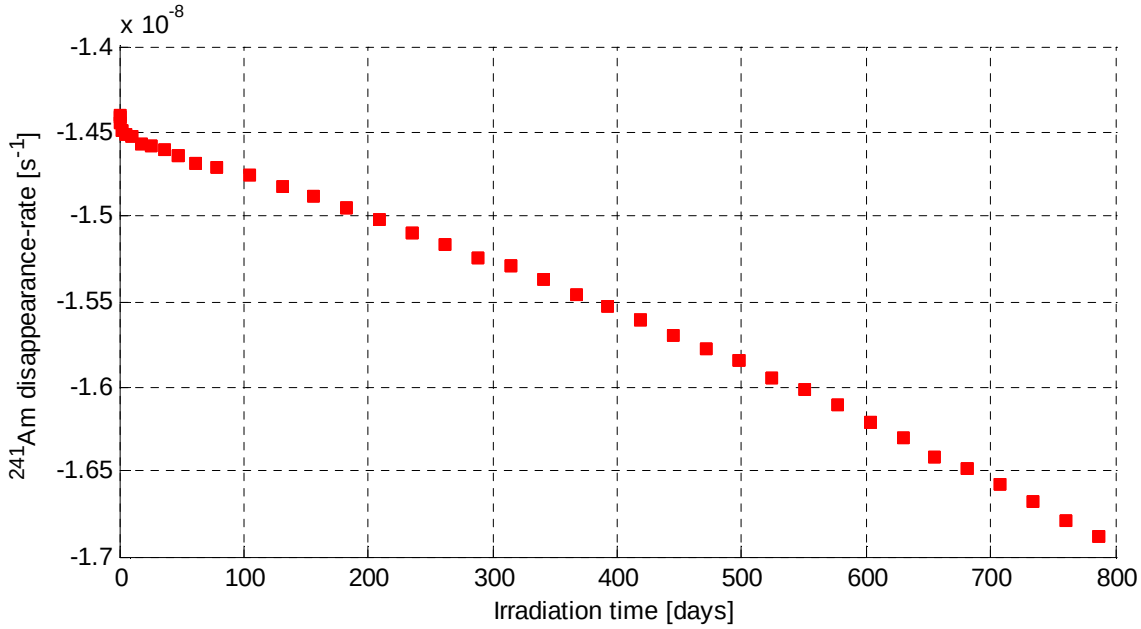

A.17 Am-242m disappearance rate evolution throughout irradiation time

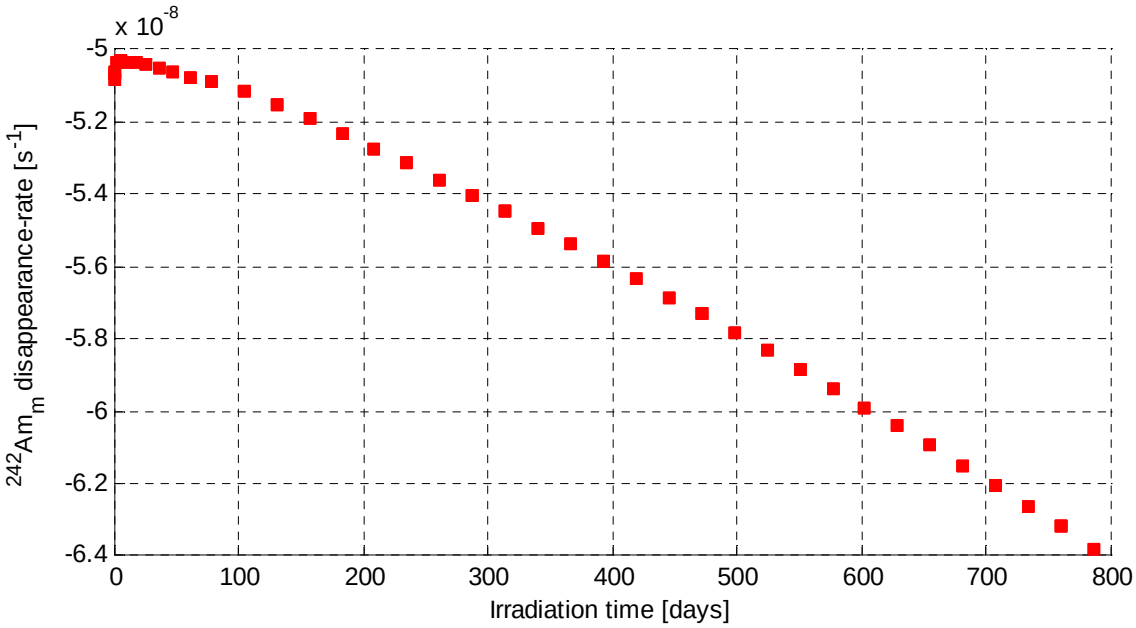

A.18 Am-243 disappearance rate evolution throughout irradiation time